Heterogeneity of free and occluded bitumen in a natural maturity sequence from Oligocene Lake Enspel

Christian J. Illing, Christian Hallmann, Andrew C. Scott, Margaret Collinson, Derek E.G. Briggs, Harald Strauss, Roger E. Summons

PII: S0016-7037(18)30607-0
DOI: https://doi.org/10.1016/j.gca.2018.10.021
Reference: GCA 10982

To appear in: *Geochimica et Cosmochimica Acta*

Received Date: 1 May 2017
Revised Date: 19 July 2018
Accepted Date: 17 October 2018

Please cite this article as: Illing, C.J., Hallmann, C., Scott, A.C., Collinson, M., Briggs, D.E.G., Strauss, H., Summons, R.E., Heterogeneity of free and occluded bitumen in a natural maturity sequence from Oligocene Lake Enspel, *Geochimica et Cosmochimica Acta* (2018), doi: https://doi.org/10.1016/j.gca.2018.10.021

(Geochimica et Cosmochimica Acta)

Heterogeneity of free and occluded bitumen in a natural maturity sequence from Oligocene Lake Enspel

Christian J. Illing[1,2,3], Christian Hallmann[4,5]*, Andrew C. Scott[6], Margaret Collinson[6], Derek E. G. Briggs[7], Harald Strauss[1] and Roger E. Summons[2]

[1] Westfälische Wilhelms-Universität Münster, Institut für Geologie und Paläontologie, Corrensstr. 24, 48149 Münster, Germany; [2] Massachusetts Institute of Technology, Department of Earth, Atmospheric and Planetary Sciences, Cambridge, MA 02139, USA; [3] Present address: Federal Agency for Technical Relief (THW) - Headquarters, Provinzialstraße 93, 53127 Bonn, Germany; [4]Max Planck Institute for Biogeochemistry, Hans-Knoell-Str. 10, 07745 Jena, Germany; [5]MARUM, University of Bremen, Building IW-3, Am Biologischen Garten 2, 28359 Bremen, Germany; [6]Department of Earth Sciences, Royal Holloway University of London, Egham, Surrey, TW20 0EX, UK; [7]Department of Geology and Geophysics, Yale University, New Haven, CT 06520, USA

* Correspondence should be addressed to challmann@bgc-jena.mpg.de

Highlights:

- Bitumen yield and composition can vary with maturity and extraction technique
- Occluded Bitumen 2 is not an artifact of incomplete extraction
- Bitumen 2 systematically exhibits higher maturities and signs of enhanced, clay-catalyzed diagenetic transformations
- During sequential extractions, successive compositions trend towards those of Bitumen 2
- Rapid high-T° maturation disproportionally affects the color of palynomorphs and Rock-Eval T_{max} values, compared to molecular maturity parameters and vitrinite reflectance.

Keywords:

Oligocene, lacustrine, extraction, Bitumen 2, maturation, pyrolysis.

ABSTRACT

Sedimentation in Oligocene Lake Enspel was rapidly terminated by a basaltic lava flow. This introduced a preservational barrier while imparting a 'natural flash pyrolysis', during which the organic matter in underlying stratigraphic units was subjected to rapid thermal maturation resulting in hydrocarbon generation. Samples from these strata exhibit a steep maturity gradient (0.25–1.07 % optical vitrinite reflectance, or R_O) over uniform organofacies. This offers the opportunity to investigate bitumen generation during rapid thermal maturation mechanistically, in particular the nature of Bitumen 2—occluded bitumen, which is only recoverable after the digestion of the mineral matrix and was frequently dismissed as an artifact of incomplete extraction. Elaborate sequential extraction of the contact metamorphic sequence of oil shales at Enspel revealed systematic changes in bitumen composition. These trend progressively towards those of occluded bitumen, which exhibits a systematically elevated thermal maturity, a higher degree of catalytic biomarker-rearrangement and the conspicuous absence of molecular signatures from vascular plants that are present in the free bitumen. One plausible explanation involves a contribution of allochthonous clay-adsorbed organic matter to Bitumen 2. This could represent a mixture of older reworked bitumen and an early-diagenetic snapshot of clay adsorbed organic matter. Alternatively, a close association of early-generated bitumen with clay minerals may have led to enhanced isomerization and catalytically influenced 'uniformization' of alkane signatures. Deviations from the expected relationships between various thermal maturity parameters suggest variable dependence on the time-pressure-temperature pathway (i.e. metamorphic facies). The maturation of organic matter likely behaves differently under a contact metamorphic regime or during rapid subsidence and exhumation, as compared to slow maturation during regional subsidence. Our data also suggest that geologically brief shallow intrusive or extrusive magmatism might not be as destructive to the sedimentary hydrocarbon inventory as hitherto thought. This study draws attention to the small-scale compositional heterogeneity of bitumen that can be studied using sequential extraction methods. More importantly, it suggests that occluded bitumen could potentially harbor information on organic matter that pre-dates *in situ* primary productivity and may be derived from allochthonous biomass and detrital input.

1. INTRODUCTION

Sedimentary hydrocarbons in the form of bitumen or—when present in larger abundances—petroleum, constitute an organic phase that is released from kerogen and differs from it in molecular size and, hence, solubility in organic solvents (Vandenbroucke and Largeau, 2007). Kerogen is macromolecular organic matter, dispersed in sediments and formed by preservation of large biomolecules (such as algaenan, sporopollenin, cutin or lignin) together with recondensation of smaller molecular units that survive early diagenesis (e.g. Durand, 1980; Tegelaar et al., 1988; Sinninghe-Damsté et al., 1998; de Leeuw et al., 2006). Research on plant and animal cuticles has revealed that labile aliphatic moieties can be incorporated into the decaying residue *in situ* during early diagenesis and contribute to the insoluble aliphatic inventory in kerogen (Briggs, 1999; Collinson, 2011; Gupta et al., 2009; Stankiewicz et al., 1996). It is this insoluble kerogen that releases bitumen at elevated temperatures and pressures due to thermodynamic instability and, in parallel, undergoes changes in its physical properties, as reflected in its three dimensional structure (i.e. porosity) and density (e.g. Vandenbroucke and Largeau, 2007; Löhr et al., 2015). One consequence of bitumen generation is an increase in internal pressure, (micro-) fracturing and, depending on the amount of bitumen generated, so-called primary migration or expulsion away from the generative kerogen (Palciauskas, 1991). Although bitumen and kerogen have been studied for decades, surprisingly little is known about the spatial disposition of bitumen and its heterogeneity within the site of generation. Yet such information could significantly enhance our understanding of the thermal preservation of biomarker hydrocarbons, biosignature contamination, and aspects of charge mixing that are of relevance to the petroleum industry.

1.1 Free and occluded bitumen, *also known as* Bitumen 1 and 2

The chemical composition of bitumen progressively released from a kerogen pool during increasing thermal maturity systematically shifts towards a composition of higher volatility, higher aromaticity, and a lower content of polars and asphaltenes. On a molecular level, the stereochemistry of many molecules approaches equilibrium of thermodynamically stable structures (Tissot and Welte, 1984; Pepper, 1991; Peters et al., 2005). Where kerogen in rock samples lacks the abundance and/or quality to

release fluids, the remaining extractable bitumen represents a mixture of early and later generated hydrocarbons, together with those lipids that were not incorporated into the macromolecular kerogen framework at the outset. Because the quantitative generative capacity of kerogen increases towards a defined thermal maturity point (the 'peak oil window'), the early (i.e. less mature) molecular signature is readily overprinted by that of more recently generated bitumen. In addition, destruction of the labile (early generated) portion of bitumen at higher maturity levels (gas window) causes the high maturity signature to be most prominent.

The sequential extraction of porous rock samples can separate early-generated phases (which, due to a higher proportion of polar compounds, may exhibit greater adsorption to the rock matrix) from more mature, later-generated phases (e.g. Schwark et al. 1997). This approach was successfully used by Kramer et al. (2004), Hallmann et al. (2006, 2007) and Arouri et al. (2009) to separate remnant bitumen from different oil charges present in individual samples. Yet the exact spatial distribution of these co-occurring bitumen phases remains obscure. Wilhelms et al. (1991) reported that extractable organic matter that remains in rock powders *after* solvent extraction (i.e. Bitumen 2) can negatively impact the reliability of Rock Eval measurements. Many studies have confirmed that the extraction of a rock sample powder is rarely exhaustive: a variably small proportion of bitumen remains within the extraction residue (e.g. Behar and Vandenbroucke, 1988; Eigenbrode, 2004; Sherman et al., 2007; Waldbauer et al., 2008; Nabbefeld et al., 2010; Holman et al., 2012). Smith et al. (1970) found that re-extraction of kerogen concentrates created by demineralization (i.e. removal of carbonates and silicates with mineral acids) frequently yields a bitumen phase that in some cases differs compositionally to that of the freely extractable bitumen. In the case of Precambrian rocks in particular, Bitumen 2 (B2) was once considered a contaminant-free phase (Eigenbrode, 2004; Sherman et al., 2007; Waldbauer et al., 2008) based on the rationale that because it is inaccessible to solvent extraction, it must also be protected from contamination. The application of this concept to rocks of Archean age yielded credible results on seemingly indigenous Archean hydrocarbons. French et al. (2015), however, showed that the thermal maturity of organic matter in different Archean sedimentary formations from the Australian Pilbara Craton, previously thought to be suitable for

biomarker analysis, is beyond the stability field of polycyclic terpenoids, implying that even the B2 signal found in these units must have been affected by contamination.

The nature of B2 remains controversial. Is it a remnant of incomplete extraction, where the second, occluded extract is much lower in concentration and more easily contaminated resulting in differential signatures? Or is it a remnant of early released bitumen that is protected by occlusion within crystals or by adsorption to kerogen and/or clay minerals? Although various authors favor the latter explanation (e.g. Wilhelms et al., 1991; van Kaam-Peters et al., 1998; Sherman et al., 2007; Nabbefeld et al., 2010; Holman et al., 2012, 2014), this question has not been unambiguously resolved. Kerogen porosity is receiving increasing attention: immature kerogen lacks pores, but a significant pore volume with diameters <5 nm develops with increased thermal maturity (Modica and Lapierre, 2012; Kuila et al., 2014). Although the initial interest in kerogen porosity was prompted by studies of gas storage capacity in unconventional reservoirs, Löhr et al. (2015) pointed out that the pores in kerogen particles accommodate bitumen generated over a significant range of thermal maturities. Although Löhr et al. (2015) did not extract such material, it is easy to envisage a complex system of pore sizes and connectivity that would sustain small-scale bitumen heterogeneity and affect extraction efficiencies. Hence it is timely to investigate this topic from a molecular perspective and extend previous studies on B2 with the aspect of changes during thermal maturation.

Nabbefeld et al. (2010) reported differences in thermal maturity and the abundance of biomarkers rearranged via clay catalysis in B1 and B2 across the Permian-Triassic boundary, which they tentatively attributed to varying TOC/clay ratios, even though the differences did not appear to be systematic (see Section 4.7). In a follow-up study, Holman et al. (2012), focusing on aromatic hydrocarbons, performed sequential Soxhlet extraction followed by B2 release on a Paleoproterozoic sample. Their study confirmed that B2 is compositionally different from all sequentially extracted B1 fractions and showed that during progressive extraction of B1, the composition of the extract changed towards that of B2. These observations are intriguing and suggest that investigating B2 in samples of differing thermal maturity might allow future studies to determine whether B2 represents an early charge from the same kerogen, a completely different phase or simply an artifact of incomplete extraction. The answer

will be relevant to interpretations of the composition and value of diagnostic parameters in extracts obtained by different approaches.

1.2 Reliably assessing thermal maturity

Increasing thermal maturation affects sedimentary organic matter in a number of ways leading to increased aromatization of the residual kerogen macerals (Durand, 1980). This process is reflected in a continuous and preferential loss of hydrogen (relative to carbon) and ultimately leads to H/C values approaching zero. On the other hand, vitrinite macerals that derive from wood and, thus, have a common chemical precursor, increase their reflectance under oil in a single wavelength of light—expressed as R_O (optical vitrinite reflectance). Vitrinite reflectance in coals is often based on several hundred readings. In sediment samples, however, due to the smaller number of vitrinite particles, values are often based on less than 10 readings. In parallel to this maturation of wood, the color of dispersed organic matter (e.g. pollen) changes from a bright yellow or orange color, through brown tones to a loss of color when OM turns black (e.g. Hartkopf-Fröder et al., 2015). Although no calibrated quantitative scale exists, the spore color index (SCI), with values ranging from 0 to 10, is frequently used as a means of assessing organic color changes and abundant examples in the palynological literature allow for a relatively precise estimation of SCI values on the basis of detailed comparison (Collins, 1990).

The source of diagnostic biomarker hydrocarbons is frequently questioned in rocks of greater geological age or elevated thermal maturity (e.g. Brocks et al., 2008, 2011; French et al., 2015; Rasmussen et al., 2008; Leider et al., 2016) and a detailed understanding of thermal history and its impact on biomarker preservability is of paramount importance for evaluating whether detected biomarkers are indigenous. Such evaluation is frequently based on geochemical or optical parameters. Screening for these parameters can obviate detailed and elaborate molecular analysis of samples that have passed beyond the field of molecular stability for polycyclic terpenoids. Determination of a reliable threshold is complex, however, as the kinetic behaviours of different organic matter properties vary and, precluding any universally applicable calibration. Rock-Eval pyrolysis (Espitalié et al., 1977) is a standard screening technique: a sample is subjected to increasing temperature in a flow of inert gas

thereby sequentially vaporizing free hydrocarbons, that is those derived from bitumen, and subsequently releasing covalently bound hydrocarbons pyrolytically, reflecting the remaining generation potential. The temperature of maximum pyrolytic release (T_{max}) provides a proxy for thermal maturation (Peters, 1986) which can be converted to calculated vitrinite reflectance values (R_C).

1.3 Bitumen distribution and thermal maturity

In this study we investigated the nature of B2 by studying both free and occluded hydrocarbons in a natural thermal maturation sequence. Oligocene maar-lake Enspel accumulated fine-grained siliciclastic sediments within the Central European Volcanic Belt (e.g. Lüniger and Schwark, 2002; Lüniger, 2002). The organic rich, lacustrine sequence was abruptly terminated by a basalt flow during the Upper Oligocene. This rapid capping resulted in exceptional preservation of the organic matter in underlying sediments. This is evident, for example, from the oldest chitin detected in fossilized beetles using gas chromatography and mass spectrometry (GC-MS: Stankiewicz et al., 1997; older chitin signals have been detected in Carboniferous strata using synchrotron based X-ray absorption spectroscopy: Cody et al., 2011) and lignin detected in leaves (Gupta et al., 2007). More significantly for this study, however, the hot lava flow induced an almost instantaneous natural "flash" pyrolysis of the organic matter within the underlying shales, leading to a maturity sequence ranging from immature organic matter (estimated R_O of 0.25 %) to relatively mature, oil-window organic matter (~1.07 % R_O) over a distance of 75 cm. Such contact metamorphism differs mechanistically from the regional metamorphism that typically affects organic matter on a basin-wide scale, where slowly rising temperatures act in concert with rising lithostatic pressure over multi-million year time scales. But the advantages for this study prevail: while facies differences on a vertical or lateral scale strongly complicate the comparison of samples representing different thermal maturities on a basin scale, the 75 cm of shales investigated at Enspel are representative of relatively uniform organic facies (also see section 4.2) and lithology during the terminal existence of the lake (Lüniger, 2002), implying that the majority of observed changes can be directly related to thermal maturation.

Similar investigations of thermal alteration in the proximity of basalt flows have been conducted with samples of Jurassic age from Scotland (Bennett and Abbott, 1999; Bishop and Abbott, 1993) but those studies focused on the organic geochemical aspect of freely extractable hydrocarbons. Here we also consider occluded hydrocarbons and additionally investigate the thermal maturation of the kerogen (using spectroscopy, elemental ratios, organic petrography, microscopy) to increase our understanding of the thermal maturation of organic matter over different pathways in time-temperature-pressure (TTP) space. The early metamorphic pathway of organic matter might affect various maturation proxies in different ways, thereby resulting in inconsistencies. An enhanced understanding of the relative behavior of different indices of thermal maturity on different pathways will improve rapid screening of sedimentary rocks for their utility in biomarker studies (Ferralis et al., 2016). Here we use a combination of bulk chemical analyses, microscopy, bulk NMR, and molecular organic geochemistry to study the parallel maturation of kerogen, free and occluded bitumen, and to shed new light on the nature of B2.

2. MATERIALS AND METHODS

2.1 Geology

Outcrops of the lacustrine Enspel Formation are located ca. 35 km east of the city of Koblenz, ca. 6 km southwest of Bad Marienberg at the village of Enspel in the Westerwald, Germany. Located at the western end of a volcanic region, the Enspel deposits accumulated in a complex maar-like caldera and tectonic graben (Pirrung, 1998; Schindler and Wuttke, 2010, 2015). The uppermost portion of the Enspel Formation has yielded well-preserved insects, fish, mammals, amphibians, terrestrial leaves and fruits (Köhler, 1998; Poschmann et al., 2010). Microscopic investigation reveals the presence of diatoms, some *Botryococcus*-like algae, dinoflagellates and other eukaryotic algae (Clausing, 1998; Herrmann, 2010). Benthic algae and submerged macrophytes are largely absent due to the anoxic conditions that prevailed in the water column and the steep slope basin geometry that led to a very narrow (sub)littoral zone. Microbial mats have been reported and may have contributed to the

predominantly amorphous organic matter found in lake sediments (Clausing, 1998). Mammalian remains (eomyid rodents) indicate an upper Oligocene age (Storch et al., 1996), which is consistent with K-Ar dating of the overlying basalt (Horn and Müller-Sohnius, 1988). Mertz et al. (2007) obtained an age of 24.9–24.5 Ma based on Laser fusion $^{40}Ar/^{39}Ar$ step heating on volcanic feldspars. In 1996 a research well was drilled near the center of the lake, revealing a total sediment fill of 140 m (Lüniger and Schwark, 2002). Sedimentological studies have reconstructed a deep meso- to eutrophic lake with a steep marginal bathymetry (Gaupp and Wilke, 1998; Schindler and Wuttke, 2015), which was estimated to have persisted for about 230,000 years (Schindler and Wuttke, 2010). The general lack of woody fragments suggests that the lake system was hydrologically confined without major inflow. The lithology consists of uniform brown to black colored organic rich laminated shales interlayered by strata representing coarser clastic redeposition of volcanic ashes (Lüniger and Schwark, 2002; Schindler and Wuttke, 2010).

2.2 Samples

The samples (Table 1) were collected from a surface excavation at Enspel. They represent the top part of uniform maar-type lake sediments with intercalated ash layers, as detailed above. In the ca. 75 cm below the capping basalt, organic matter (OM)-rich shale accumulation was repeatedly interrupted by the deposition of six ashfall layers. In this study the basalt was defined as Level 1, while the ash layers below were given increasing odd numbers (Levels 3 to 13). Samples were obtained from each of seven intervening shale layers denoted by Levels 2 to 14, with higher numbers corresponding to increasing distance from the lava flow (Fig. 1).

2.3 Methods

2.3.1 Sample workup and preparation

The sample workup procedure, adapted from Hallmann et al. (2011), was conducted in the Geobiology Laboratory at the Massachussetts Institute of Technology. Samples were surficially cleaned and rinsed in methanol to remove external contaminants. Rocks were crushed with a hammer and powdered using a SPEX shatter box with a

stainless steel puck mill, as described in Sherman et al. (2007). Powders (10.7–37.5 g) were weighed into pre-cleaned 250 mL Teflon bottles and sequentially extracted ten times by ultrasonic agitation with dichloromethane/methanol (initially 150 mL then 100 mL; 93:7 vol:vol) at elevated temperatures (~50°C), where the temperature resulted from the ultrasonic agitation energy. Each extraction step was performed twice for 30 minutes with extensive shaking before and between steps. Suspensions were allowed to settle overnight and the supernatant solvent was decanted into beakers and pooled (extract termed ULTRA). To avoid possible contamination and evaporative losses, extracts were allowed to dry under normal atmospheric conditions at room temperature. While this can pose a problem for organic lean samples (Illing et al., 2014) the Enspel extracts are exceptionally rich in OM and are not at risk of contamination by laboratory aerosols. Since the extracts were still colored after ten extraction steps by ultrasonic agitation, we decided to continue the extraction process by pressurized liquid extraction at elevated temperatures in a *Dionex* Accelerated Solvent Extractor 300 (ASE). The extraction was performed a further 13 times using dichloromethane (DCM) and methanol (MeOH) (90:10; v:v) and extracts were pooled to obtain 6 sequential fractions (ASE-1 to ASE-6) as shown in Fig. 2.

Extraction residues (3.2–18.3 g) were loaded into pre-cleaned 50 mL Teflon centrifuge tubes for demineralization. Carbonates were digested with HCl_{aq} (6N) and subsequently rinsed repeatedly with deionized water to remove liberated cations and to prevent the *de novo* formation of fluorides upon contact with hydrofluoric acid (HF), with which the samples were subsequently allowed to react until silicates were removed. After thorough neutralization, drying and homogenization, kerogen concentrates were re-extracted 4 times with DCM by ultrasonic agitation, as described above, yielding the occluded bitumen that is B2.

All bitumen fractions were desulfurized with activated copper granules. Asphaltenes were removed by centrifugation after precipitation by adding a copious excess of *n*-hexane to samples dissolved in a minimum volume of DCM, and stored overnight at 4ºC in the dark. Maltenes were fractionated by open column chromatography (8 mL SPE glass columns) on silica gel, resulting in a saturated hydrocarbon fraction (eluted with 0.5 column dead-volume of *n*-hexane), an aromatic hydrocarbon fraction (eluted with 2 column dead-volumes of *n*-hexane/DCM 7:3) and a polar fraction containing

nitrogen, sulfur and oxygen (NSO)-compounds (eluted with 2 column dead-volumes of DCM/methanol 1:1). Fractions were concentrated at room temperature, avoiding evaporation to dryness, spiked with the internal standard d_4-ergostane (saturates) and analyzed by GC-MS.

2.3.2 Gas chromatography and mass spectrometry

The molecular compositions of the bitumen samples were analyzed at MIT where aliquots of one microliter were injected in splitless mode into an Agilent 6890 GC equipped with an HP6890 Autosampler coupled to an Agilent 5975 MSD. The GC was fitted with a DB-1 MS (saturated hydrocarbons) or DB-5 MS (aromatic hydrocarbons) capillary column (both of 60 m length, 0.25 mm inner diameter, 0.25 μm film thickness) and helium was used as a carrier gas with a constant flow of 1 mL/min. The temperature program started at 60ºC (isothermal for 2 minutes), ramped at 3.5º/minute to 335ºC, and was held isothermal at final temperature for 19.4 minutes. Analytes were ionized by electron impact at 70 eV and detected both in full scan (*m/z* 50–550) and selected ion monitoring (SIM; *m/z* 85, 83, 191, 217, 221 for alkanes, acyclic isoprenoids, hopanes, steranes and the internal standard). Tricyclic terpenoids, hopanes and steranes were additionally analyzed via metastable reaction monitoring (GC-MRM-MS) using a Micromass Ultima Autospec MS coupled to an Agilent 6890N GC as described by Illing et al. (2014). Quantification of analytes was performed relative to the internal standard without correcting for individual response factors.

2.3.3 ^{13}C Solid state NMR spectroscopy

All nuclear magnetic resonance (NMR) experiments were performed on a Bruker Avance 400 MHz NMR spectrometer operating at 100.61 MHz for ^{13}C at the University of Bristol. High Power Decoupling (HPDEC) experiments were carried out using a standard HPDEC pulse sequence with high-power composite-pulse ^{1}H decoupling employed during the acquisition of the ^{13}C FID. The samples were analyzed applying Magic Angle Spinning at a rate of 10.450 kHz. A ^{13}C $\pi/2$ pulse time of 3.5 μs

and a recycle delay of 120 s between scans were used for all the samples to obtain quantifiable integrals.

2.3.4 Organic matter color and reflectance

Microscopic studies were conducted at Royal Holloway, University of London, where sediments were studied as 'blind samples' with unidentified stratigraphic position. Polished blocks and thin sections (both perpendicular to bedding) were used for photomicroscopy and for reflectance studies. Part of the sediment was prepared using standard palynological techniques (treatment with HCl and HF only). Strew slides of the resulting organic matter preparations were devoid of suitable spores or pollen, and the thermal alteration was estimated by visual comparison of the color of concentrated organic matter to the color chart published by Traverse (1988, top of plate 1, p. 426a). This chart was used to give a color descriptor (yellow, orange, brown to black) and to provide a numerical value, ranging from 1 (palest color) to 10 (darkest color).

The reflectance of organic matter was measured on polished sediment blocks (perpendicular to bedding) under a Nikon Microphot microscope using Leica QW in image analysis software. The specimens were measured under Cargill immersion oil (refractive index of 1.518 at 23°C) using a 40x objective lens. A range of standards was used for calibration: cubic zirconium (R_O 3.19 %), GGG (R_O 1.75 %), YAG (R_O 0.93 %) and Spinel (R_O 0.39 %). The light source was a Nikon fibre optic LS-101 and a filter allowed the use of 546 nm light for reflectance measurements. For each of the samples 25 random points were measured (where possible); the mean random reflectance was obtained and the 2x standard error was calculated. Photo micrographs were taken with a microscope mounted Nikon digital sight DS-5M camera head and DS-L1 controller with either 1280 x 960 or 2560 x 1920 pixel resolution.

2.3.5 Elemental analyses

C, H and N abundances were determined with a Carlo Erba EA 1108 at the University of Bristol. The amounts of carbon (present as carbonate) and sulfur were determined with a Coulomat 702 (Strohlein). The total organic carbon (TOC) was determined by subtracting the amount of carbon present as carbonate from the total amount of carbon.

All values are averages of duplicate measurements and have an average reproducibility of ± 0.2 %.

2.3.6 Programmed pyrolysis screening

For the commonly applied programmed pyrolysis method a Rock Eval 6 (Vinci Technologies; Lafargue et al., 1998) was used at the Federal Institute for Geosciences and Natural Resources, Hannover, Germany. The thermal maturity (T_{max}) and organic matter quality (S1: free hydrocarbons in mg/g TOC; S2: covalently bound hydrocarbons in mg/g TOC) were determined on untreated and on pre-extracted powders according to Espitalié et al. (1977). The method was calibrated against the IFP550000 standard and results have been corrected to account for differing sample weights.

2.3.7 X-ray diffraction (XRD) analyses

Dried bulk samples were ground to a fine powder (<20 µm particle size) and prepared with a Philips backloading system. The X-ray diffractograms were obtained at the University of Bremen (Central Laboratory for Crystallography and Applied Material Sciences, ZEKAM, Dept. of Geosciences) on a Philips X'Pert Pro multipurpose diffractometer equipped with a Cu-tube (k_α 1.541, 45 kV, 40 mA), a fixed divergence slit of ¼°, a 16 samples changer, a secondary Ni filter and the X'Celerator detector system. The measurements were performed as a continuous scan from 3–85° 2θ, with a calculated step size of 0.016° 2θ (calculated time per step was 50 seconds). Mineral identification was achieved by means of the Philips software X'Pert HighScore™ and sheet silicates were identified with the freely available Apple MacIntosh X-ray diffraction interpretation software MacDiff 4.25 (Petschick et al., 1996). This was followed by full quantification of the mineral assemblage of the bulk fraction via the QUAX full pattern method (c.f. Vogt et al., 2002).

2.3.8 Reproducibility of data

All data were collected on single, individual samples, and not on replicates, as sometimes done in organic geochemical studies where completely new methodologies

are being tested. The methodologies we used are standard procedures in organic geochemistry and have been documented in numerous studies from our laboratories (e.g. Grosjean et al., 2009) and which have been evaluated in inter-laboratory comparisons in the past (e.g. Rullkötter and Isaacs, 2001). The molecular geochemical trends trends reported in this manuscript are internally consistent and corroborated by Rock-Eval pyrolysis data and microscopic observations.

3. RESULTS

3.1 Bulk composition of samples

3.1.1 Elemental CHN composition

The carbonate content is consistently very low in all samples, ranging from 0.015 to 0.025 wt.% (average 0.024 wt.%; Tab. 1). The total organic carbon content (TOC) of samples varies from 3.5 to 24 wt.% with a systematic decrease from 12.7 wt.% in the (lowest) Level 14 to 3.6 wt.% in Level 2 closest to the lava flow. A conspicuous exception occurs at Levels 6 and 8 with values of 23.5 and 24.0 wt.%, respectively. The absolute concentration of nitrogen decreases with increased thermal overprint (i.e. towards the lava flow) in parallel with the carbon content. The overall systematic decrease from 0.35 wt.% N in Level 14 to 0.05 wt.% N in Level 2 (Table 1) is disrupted by anomalously high values in Levels 6 and 8 (0.71 and 0.75 wt.%, respectively), coincident with the elevated TOC. While the C and N trends are similar, the ratio of C/N changes from around 30–37 (Levels 6–14) to ~80 (Level 2; see Fig. 1 & Tab. 1), indicating that N is preferentially lost at a high maturity (e.g. Vandenbroucke and Largeau, 2007). The range of C/N values is consistent with a terrestrial plant input, which typically yields C/N values of 20–100 (Meyers and Ishiwatari, 1993; lacustrine algae have characteristically low values of 5–8). This is in accordance with the findings of Lüniger and Schwark (2002), who concluded that much of the Enspel organic matter is derived from land plants.

3.1.2 Aromaticity

The total aromaticity (δ) as determined by ^{13}C NMR represents the ratio between the abundance of aromatic carbon and total carbon in a sample and gives an indication of thermal maturity (Mitchell, 2001). The NMR spectra of samples from Level 2 and Level 14 reveal a distinct increase in the aromatic signal in the 100–150 ppm region (Fig. 3). The aromaticity exhibits a roughly systematic stratigraphic trend with highest values (0.487 and 0.547, respectively) in the samples close to the lava flow (Levels 2 and 4) and the lowest value (0.267) in the most distant sample (Level 14). The intervening samples show a trend of increasing aromaticity with the exception of the sample from Level 12, whose value (0.402) is elevated from the trend.

3.1.3 Organic matter color and reflectance

Organic matter color and vitrinite reflectance were determined on all samples. The color darkens from orange brown and dark orange brown (color numbers 4 to 5) in the layers most distant from the lava flow (Levels 10 to 14), via very dark orange brown (number 7) in Level 6 to black (numbers 9 to 10) in Level 2 (Fig. 4). The color trends are more reliable than the individually assessed colors. Matching organic matter color and vitrinite reflectance data must be approached with caution. The measured reflectance of vitrinite macerals (R_O; Taylor et al., 1998) increases systematically from values of 0.25 % in the lowest levels (Level 14) to 1.07 % in Level 2. The highest figure (1.07 %) is based on two measurements only (as opposed to 25 for other samples) and must be considered an indication rather than a robust value. These R_O values correspond to a range from the field of diagenesis to the peak/upper oil window (e.g. Hartkopf-Fröder et al., 2015). Both organic matter color and vitrinite reflectance show a major change as the lava flow is approached.

3.1.3 Programmed pyrolysis screening

Thermal maturity, as defined by the temperature of maximum hydrocarbon release during Rock Eval pyrolysis (i.e. T_{max}) ranges from values around 430–435º in the least mature samples (Levels 8 to 14), via elevated values of ~445º in Level 6, to highly mature values in Levels 2 and 4. While the less mature Levels 6 to 12 exhibit very similar T_{max} values for solvent-extracted and unextracted samples (Table 1, Fig. 1), a systematic offset is evident in the most mature Levels 2 and 4: here T_{max} values

of extracted samples are consistently lower (490º and 484º, respectively) than those of unextracted samples (520º and 514º). S2 values of extracted samples, representative of remnant hydrocarbon generation potential overall, increase to a maximum of 124.51 mg/g TOC at the oil generative window in Level 8 and then rapidly decrease to values of 0.11 mg/g TOC (Level 4) and 0.03 mg/g TOC (Level 2). Results of the Rock Eval Analysis are listed in table 3.

3.1.3 XRD composition

The bulk mineralogical composition of studied samples (Table 4) reveals that all are largely dominated by expandable clays (36.0–63.6 %). Carbonates are <3% in all studied samples, while pyrite abundances are mildly elevated in those levels with elevated TOC content (i.e. Levels 6 and 8) as well as in Level 14. A large variation in quartz content (2.4–49.8 %) is observed. None of the mineralogical observations correlate internally and no systematic stratigraphic trend is obvious.

3.2 Geochemical results

3.2.1 Bitumen yield

Gravimetric analysis revealed that ultrasound-assisted solvent extraction of bitumen (ULTRA) yielded (Fig. 5c) between 0.045 mg/g (Level 2) and 26.620 mg/g rock (Level 6). Given that the extracts, except those of samples from Levels 2 and 4, were still strongly colored after 10 extractions, we switched to Accelerated Solvent Extraction (ASE) and performed 13 further extractions that were pooled into 6 fractions (named ASE 1–6; see Fig. 2 for a scheme). Levels 6 and 8 generally yielded the highest extract abundances, corresponding to the elevated TOC content in these levels. Overall, summed ASE yields ranged from 0.307 mg/g in Level 2 to 6.477 mg/g rock in Level 14 (Fig. 5c). The ULTRA contribution to total summed extracts varied systematically from ~12 % in Level 2 up to ~75 % in Level 6 and subsequently decreased to ~49 % in Level 14 (Fig. 5a). The yield obtained by individual sequential ASE extraction steps varied between the more mature samples (Levels 2 and 4), which showed a rather constant yield decreasing only towards the end (Fig. 5b). The less mature Levels 6 to 14 were more readily extracted to exhaustion: here 50 % of

the summed total ASE extract was already obtained after 5 extraction steps; 90 % after 11 steps. The extraction of kerogen concentrates yielded (Fig. 5c,d) B2 fractions of 0.026 (Level 2) to 4.485 mg/g rock (Level 14). The absolute abundance of B2 decreases with increasing thermal maturity, and the relative amount of this B2 to the total extract (summed ULTRA and ASE) is ~7 % to ~21 % with a decreasing trend towards higher maturities. Bitumen yields are tabulated in Supplementary Information (SI Table 1).

3.2.2 Molecular composition of the bitumens

Varying with the degree of thermal maturity, all saturated hydrocarbon fractions in both free bitumen (ULTRA, ASE) and in B2 were dominated by either *n*-alkanes (Levels 2–4) or hopanoids (Levels 6–14). Hopanoid abundances generally decreased with increasing thermal maturity, while alkane chain lengths and the alkane maximum increased (Fig. 6). This trend of increasing average alkane chain length was observed in both free bitumen and B2, and suggests that no significant thermal cracking of bitumens has occurred. The range in alkane chain lengths and alkane maxima also differs systematically between free bitumen (ULTRA) and B2 (Fig. 6): apart from the Level 4 sample, B2 alkanes are always shifted to higher molecular weight homologs relative to free bitumen. A pronounced odd-over-even dominance, manifested in the *n*-C_{23} to *n*-C_{33} region, was observed only in the least mature samples (ULTRA, ASE) and was conspicuously absent from any of the B2 extracts. The CPI (calculated for the range from *n*-C_{24} to *n*-C_{34} after Bray and Evans, 1961) varied between values of 8.9 in Level 12-14 and 1.3 in Level 2.

Monounsaturated alkenes with unspecified double bond position were present in most of the ASE extracts with decreasing abundances towards higher maturities, but absent in the most mature samples (Levels 2 and 4). They were also largely absent from the ULTRA extracts, with the exception of the sample from Level 6. Monounsaturated alkenes in B2 exhibit a trend towards lower concentrations with increasing thermal maturity. With progressive sequential ASE extractions, the yield of alkenes decreased, but more slowly than the decrease in alkanes. This suggests that the abundance ratio of alkenes/alkanes increased systematically during successive extraction steps, possibly indicating a tighter adsorption of alkenes to the mineral matrix. Yet the

alkene/alkane ratio in subsequent B2 extracts does not follow this trend and exhibits lower values. In contrast to the *n*-alkanes, whose average chain length (ACL; weighted average covering chain lengths from nC_{20} to nC_{40}) increases with increasing thermal maturity, the alkene-ACL (covering $nC_{15\text{-ENE}}$ to $nC_{39\text{-ENE}}$) of both ASE and B2 extracts remained roughly invariant throughout different maturity stages. However, with progressive ASE extractions, the difference in ACL between alkanes and alkenes decreased systematically and this trend continued into the B2 extracts: e.g. in Level 6 the ASE-1 extract displays $ACL_{\text{-ANE}}$ of 28.5 *vs.* $ACL_{\text{-ENE}}$ of 24.0, whereas the B2 exhibits ACL values of 24.3 (-ane) and 23.5 (-ene). These values reflect the variable ACL of alkanes, not alkenes.

Hopanes were present in varying abundances in all studied samples and extracts (Fig. 7). In a stratigraphic context, the overall abundance of summed hopanes decreases somewhat erratically with increasing thermal maturity from values of 4.2 mg/g rock (33.11 mg/g TOC) in Level 14 to ~0.0013 mg/g rock (0.036 mg/g TOC) in Level 2. From the perspective of extraction efficiency, the relative abundances of hopanes were generally highest in the ULTRA extracts: 94.5 to 99.9 % (average of 98.4 %) of all free hopanes (summed ULTRA and ASE) were recovered during this first, relatively mild ultrasound extraction step. In addition, B2 released a further 0.3 to 31.3 % (average 11.75 %; normalized to the summed ULTRA and ASE), indicating that a significant proportion of the hopanes is present in occluded form and cannot be recovered without removal of the mineral matrix. In terms of the molecular distribution, immature samples are dominated by 17β-trisnorhopane (17β-C_{27}) and by ββ-hopanes. With increasing maturity, their abundances decrease, while 18α(H)-22,29,30-trisnorneohopane (Ts) and 17α(H)-22,29,30-trisnorneohopane (Tm), as well as αβ- and βα-hopanes (moretanes), increase (Fig. 8a). For the immature samples, B2 hopanes differ from those recovered in ULTRA by a significantly enhanced abundance of 17β-C_{27} hopane and slightly lower abundances of moretanes. Counter to expectations, this stronger 17β-C_{27} signal remains characteristic of B2 hopanes even at elevated maturities. Bitumen-2 hopanes of intermediate and elevated maturity also exhibit systematically elevated αβ/βα ratios for C_{29}–C_{31} homologs, pointing to either a higher thermal maturity or an enhanced isomerization due to intrinsic parameters. Independent of these stereochemical changes, ββ-hopanes, αβ-hopanes and βα-hopanes in free extracts (ULTRA) of all thermal maturity levels exhibit C_{29}/C_{30} ratios

<1. B2 extracts of all maturity levels consistently exhibit C_{29}/C_{30} ratios >1, suggesting that the relative abundances of C_{29} and C_{30} hopanes are not affected by thermal maturation alone but probably stem from the characteristics of their biohopanoid-precursors.

Steranes were generally present in low abundances. The carbon number distributions are mostly dominated by stigmastane (C_{29}: 31–63 %; mean 45.5 ± 7.5 %) and cholestane (C_{27}: 24–47 %; mean of 32.7 ± 5.9 %) isomers with lower abundances of ergostanes (C_{28}: 9–42 %; mean 21.8 ± 9.0 %) (Fig. 8b). The main variability appears to be between stratigraphic levels, but significant variation is also observed between the B1 and B2 of individual samples. The difference between B1 and B2 is roughly constant, regardless of the increasing maturity. In B2 C_{29}-sterane is still the dominant homolog (31–49 %; mean 39.5 ± 6.3 %; compared to 49.7 ± 8.2 % in ULTRA), but the abundances of C_{27}-steranes (27–47 %; mean 34.3 ± 7.0 %) and C_{28}-steranes (9–42 %; mean 26.1 ± 12.2 %) are higher. Progressive stereoisomerization was observed with increasing thermal maturity in all samples for all homologs, but striking and systematic offsets were present: B2 appeared to be consistently more mature than B1 (ULTRA), with the exception of the C_{27} αββ/ααα+αββ ratio for Levels 6 and 8. Furthermore, relative abundances of diasteranes were consistently low in B1 (ULTRA, ASE), but elevated in B2 (Fig. 9).

Tricyclic terpenoids ranging from C_{23} to C_{26}, as well as a C_{24} tetracyclic terpane, were observed in all samples. Tricyclics increased in abundance relative to hopanes with increasing thermal maturity whereas the relative abundance of the tetracyclic compound decreased slightly from Level 14 to Level 6. The reason for the low relative abundance of tricyclics and the C_{24} tetracyclic compound, as compared to hopanes, in Level 2 is obscure but may indicate a distillation process. The molecular compositions discussed above are tabulated in the Supplementary Information (SI Table 2).

Aromatic hydrocarbons were present in generally low abundances and are the subject of a separate study. Specifically diagnostic isoprenoidal hydrocarbons, such as pentamethylicosane, crocetane or aryl isoprenoids, were not detected in any of the studied samples.

4. DISCUSSION

4.1 Calibration of kerogen and bitumen maturity parameters

Reflectance values for the Enspel sequence varied from 0.25 to 1.07 % R_O, equivalent to a T_{max} of <420–457°C (after Jarvie et al., 2001) and ranging from immature OM up to the late peak oil window (Peters and Cassa, 1994). This stands in contrast to measured T_{max} values (Table 2), which are consistently higher than expected from optical reflectance analysis: less mature samples in Levels 12 to 14 afford values around 430ºC and the most mature samples in Levels 2 and 4 afford values significantly higher than the reflectance-estimated 457ºC—i.e. up to and beyond 500ºC (Fig. 1). Thus either reflectance underestimates thermal maturity in these samples, or Rock Eval measurements overestimate it. In terms of coloration, an SCI of 2 to 8 is predicted by a recent correlation of different maturity parameters (Hartkopf-Fröder et al., 2015). The colors of palynological organic matter within the studied sample set range from ~4 to 9/10. The darkest colors (black, 9 and 10) should correlate to ~2 % R_O and a dry gas window maturity, according to Hartkopf-Fröder et al. (2015). This is more in line with measured T_{max} values and higher than maturity estimates on the basis of measured optical reflectance. Could the chemical conversion of vitrinite macerals be mechanistically slower than the other analyzed parameters, leading to a maturity underestimation by vitrinite reflectance when thermal maturation occurs rapidly under a high temperature regime, as at Lake Enspel? Given the inferences based on color and T_{max} values, diagnostic polycyclic hydrocarbon biomarkers should not have survived in these most mature samples (i.e. Levels 2 and 4). Yet they are abundantly present. For the measured maturity range of 0.25 to 1.07 % R_O, molecular isomerization ratios in steranes (both 5, 14, 17 αββ/(ααα+αββ) and 20 S/(S+R)) and hopanes (17, 21 αβ/(αβ+βα) and 22 S/(S+R)) should range from values near zero to the maxima attainable for the individual parameters (Peters et al., 2005; Killops and Killops, 2005), yet this is not the case (Fig. 10). There is a major discrepancy between thermal maturity estimated by Rock Eval pyrolysis and organic matter color *vs.* molecular parameters, and this anomaly appears larger for the less mature samples (Fig. 10). The Rock Eval data reveal a further aberration: in Levels 2 and 4 the T_{max} values of solvent-extracted samples are significantly lower (490º and

484ºC) than those of samples that were not solvent extracted (520º and 514ºC). Although it should be noted that polycyclic biomarker hydrocarbons would not be expected to have survived at any of these maturity levels, the observed offset is large, consistent and significant. While the solvent-extracted samples (i.e. the lower T_{max} values) should reflect the true thermal maturity, the question of how a solvent-extractable phase that should not contribute to the T_{max}-determining S2 peak can skew T_{max} to higher values remains enigmatic (free hydrocarbons, i.e. all solvent-extractable bitumen, are removed by Rock Eval thermolysis as the so-called S1 peak). A putative explanation is a refractory asphaltenic phase, which remains soluble—and removable—in conventionally employed solvents yet is of too large a molecular size to volatilize with other 'free' hydrocarbons. Instead this phase must release hydrocarbons pyrolytically at highly elevated temperatures, resulting in higher T_{max} values. It is likely that this asphaltene contribution to S2 and T_{max} occurs in all samples, but only becomes detectable or significant as soon as the production capacity is depleted due to thermal maturation. This is evident from the size of the S2 peak (extracted samples), which amounts to 0.03 and 0.11 mg/g TOC in Levels 2 and 4, respectively, but is significantly larger (75.5 and 124.51 mg/g TOC in Levels 6 and 8, respectively) in less mature samples. However, a detailed explanation of the underlying cause is subject to future research.

4.2 Lithology, mineralogy and depositional facies

Within the studied interval of ~75 cm the black shale layers constitute <50%, the remaining material representing primary or reworked ash deposits that are considered to have been deposited almost instantaneously (Lüniger, 2002). Assuming a slow rate of sediment deposition (e.g. 6 m/Myr) that may explain the elevated TOC contents, the studied section would have been deposited well within ~54 Kyr. No major climatic change would have occurred during the accumulation of the studied sediment package. From our knowledge of the geochemistry (e.g. Lüniger 2002) and palynology (Herrmann, 2007, 2010) of the complete lake deposit, the upper one meter can be regarded as highly uniform in its recording of rather invariant ecology. Pollen of *Inaperturopollenites concedipites*, for example, comprises a visually estimated 4.5–8.0 % of all pollen in the upper 1 m of the Enspel depositional sequence, whereas this visually estimated value varies between 0 % and 47 % throughout the full

sequence (Herrmann, 2007) and most pollen-based reconstructions of biological changes reveal a periodicity of floral fluctuation that is much larger than the studied 75 cm. The periodic fluctuation of principal algal primary producers—in this case *Botryococcus vs.* dinoflagellates—fluctuates with an even larger periodicity (Herrmann, 2007).

All studied black shale samples exhibited a highly similar visual lithology. Yet mineralogical analyses by XRD revealed relatively strong compositional differences between samples. In particular the relative abundances of quartz, plagioclase and to a lesser degree expandable clays vary unsystematically throughout the studied stratigraphic section. Given the short time of deposition we can exclude a shift in clastic provenance or differential climatic effects on clay mineral formation. The studied black shale horizons were intercalated between volcaniclastic horizons; we interpret the variable mineralogical composition to be a result of varying contamination of shales with these volcaniclastics. Neither the overall abundance of clay minerals, not the composition of clays, appear to correlate systematically with any other geochemical parameter, which may partially be due to the limited number of samples used in this study.

Overall a uniform organofacies is important because it enables us to attribute observed molecular changes principally to processes associated with thermal maturation and expulsion. While it is nearly impossible to obtain a sedimentary sequence covering a wide range of thermal maturity with completely invariant organofacies, the Enspel deposits come very close to meeting this requirement. Nevertheless it is clear that, although slight variation in depositional redox or organofacies cannot explain the large trends observed and described here, they may contribute to smaller deviations from expected values.

4.3 Time-Pressure-Temperature pathways of thermal maturation

In this study we observe that individual molecular maturity parameters do not behave as predicted by previous studies of organic matter in petroliferous basins. Maturity parameters are typically based on source rocks that are affected by the initial stages of regional heating as a consequence of basin subsidence—the OM is altered as

temperatures and pressures gradually increase over multimillion year timescales (Peters et al., 2005). In petrological terms, this corresponds to the zeolite–greenschist–amphibolite pathway of metamorphic facies that takes place under a 'typical' geothermal gradient. The Enspel sample set, in contrast, was affected by contact metamorphism, corresponding to a steep-T° zeolite–hornfels pathway. Significant temperatures acted over a short period of time and the pressure component was negligible due to absence of any overburden. It has been suggested that different time-temperature paths will lead to the same thermal maturity for individual samples (Harris and Peters, 2012) but this hypothesis is not consistent with our results as not all maturity indicators responded in the expected way. In the case of the organic matter color, the original correlation to % R_O by Fisher et al. (1980) fits more closely with our observations. Collins (1990), in contrast, argued that SCI is highly dependent on specific thermal history, and showed a steeper correlation between SCI and % R_O values (i.e. stronger increase of SCI per unit % R_O). Our analyses of the Enspel hydrocarbon inventory show that it is much less affected by thermal maturation than would be expected from either its organic matter color or measured vitrinite reflectance. The presence of higher water content in pores or adsorbed to the minerals may induce a self-limiting effect upon overpressuring by heating (e.g. Uguna et al., 2016). Irrespective of the mechanism, it is clear that no universal calibration is possible between the various parameters of thermal maturation and metamorphic facies. In practical terms, the implication is that shallow intrusive and extrusive magmatism is not as destructive to the sedimentary hydrocarbon inventory as originally thought, and that the color of organic matter is not always a good indicator of biomarker preservation: dark coloration in a rapidly subsiding and exhumed basin may still be accompanied by some hydrocarbon preservation.

Magmatic intrusions may exhibit a positive migration bias towards softer lithologies, including source units, which could lead to unusual maturity values in the organic fluids generated. Although more work is needed to understand the time-temperature-pressure details of the thermal maturation of organic matter, this aspect of organic geochemistry may become more important in explaining frequently observed discrepancies or oddities in the observed thermal maturity of bitumen and kerogen.

4.4 Extraction efficiency of free bitumen

Bitumen, i.e. the solvent-soluble fraction of sedimentary organic matter comprised of molecules not covalently bound to the kerogen macromolecular network, is continuously released during progressive thermal maturation of kerogen. Its composition is thought to reflect the maturity point at the time of generation (Tissot and Welte, 1984). Early generated bitumens tend to consist of larger molecules and are enriched in components containing polar N, S and O atoms, whereas mature late-stage bitumens become increasingly dominated by hydrocarbons and exhibit a general shift towards smaller molecules (Tissot and Welte, 1984). This difference reflects the gradual transition to the generation of condensates and, eventually, gases. Furthermore, extraction of bitumen with organic solvents is widely considered to be straightforward: repeated extraction steps—performed to increase the total extract obtained—should yield bitumens of the same or similar composition. Similarly, while the extraction efficiencies of various techniques (e.g. Soxhlet, ultrasound-assisted extraction, microwave-assisted extraction, automated accelerated solvent extraction under elevated P & T) are known to differ, the composition of extracts is often thought to be comparable in broad terms even though the literature reveals that this is not the case. Leythaeuser et al. (2007), for example, noted small-scale compositional heterogeneities in reservoir rocks, which they attributed to preferential adsorption of more polar moieties in early oil charges that remained within the host rock as successive layers of residual oils. But the same process also occurs in source rocks (e.g. Leythaeuser and Poelchau, 1991). Furthermore, bitumen generation is paralleled by both compositional and structural changes in the kerogen—in particular an increase in porosity (Löhr et al., 2015)—while volumetric expansion due to bitumen release also impacts its structure (e.g. Littke et al., 1988; Leythaeuser et al., 1988). It is therefore highly likely that a portion of the bitumen will remain within this porous network or become trapped by secondary mineralization. This idea is supported by the extraction of coals with pyridine, which causes swelling of the kerogen and can increase the extract yield by up to 50 wt.%; the efficiency of extraction depends strongly on temperature and the initial composition of samples (Van Krevelen, 1993).

In this study we employed multiple extraction techniques in sequence, with the aim of accomplishing complete extraction of free bitumen. An unanticipated consequence was the observation of striking compositional differences between sequential extracts.

Independent of elevated TOC in Levels 6 and 8, the summed TOC-normalized free bitumen yield (i.e. excluding B2, the occluded bitumen) increased systematically from 1.57 mg/g TOC in the least mature Level 14 to a maximum of 9.29 mg/g TOC in Level 8 (9.07 in Level 6) before rapidly dropping to values of 0.37 and 1.38 mg/g TOC in the most mature Levels 4 and 2. This pattern reflects the transition of sedimentary organic matter through the oil window, reaching a generative peak in Levels 6 and 8 and then experiencing progressive destruction, likely through conversion of the bitumen to smaller hydrocarbons and gases that were lost by diffusion. The reason for an extract yield increase in Level 2 is unknown but corresponds to a slightly lower aromaticity of bulk OM in this level compared to Level 4. Possible explanations include slight differences in original OM type or some secondary migration from below.

The extraction of all samples solely by ultrasonication, involving 10 individual pooled extractions, would not have yielded a representative picture in either qualitative or quantitative terms. The contribution of ULTRA to the total extract yield increased with increasing maturity towards the oil window—from around 49 % in least mature Level 14 to ~75 % in Level 6—but decreased rapidly above to about 12 % in Level 2. The decreased ULTRA yield is compensated by an increase in ASE yield in these two samples. This pattern implies a close relationship between ULTRA bitumen extracts and *in situ* generated bitumen, but raises the question why freshly generated bitumen, i.e. as a consequence of the lava flow, is 'easy' to extract and ends up in the ULTRA fraction but not the ASE extract (see Section 4.6). Our results also show that the extraction of bitumen with ultrasound may lead to severe quantitative and qualitative bias. The 13 individual ASE extraction steps were pooled into six sequential fractions (Fig. 2) and analyses revealed a general trend of progressively decreasing yields. Detailed scrutiny (Fig. 5b), however, revealed a dichotomous pattern between ASE extracts from Level 2 and 4 (most mature) and all others. Less mature samples were more rapidly extracted and yielded about 40 % of the total summed ASE bitumen during the first extraction (ASE-1), whereas the corresponding value for Levels 2 and 4 was slightly less than 15 %. This observation reflects the fact that more of the total extract of less mature samples ends up in the ULTRA fraction. The last ASE extraction step (ASE-6, Fig. 5c) yielded between 0 and 6 mg of hydrocarbons, whereas the yield of subsequent B2 extraction—separated from the last ASE step by

HCl/HF digestion of all minerals—was always higher. This supports the contention that the mineral matrix represents a barrier to extraction, but does not exclude the possibility that the B2 yield might be an artifact of incomplete extraction (but see Section 4.5).

The abundance of B2 decreased systematically (with the exception of Level 12) through the maturity sequence, counter to our expectation based on the increase in kerogen porosity with thermal maturation. This decreasing trend indicates that bitumen is not added to the occluded fraction during the transition through the oil window and raises questions about the underlying reasons. Is bitumen heterogeneity paralleled by kerogen heterogeneity? Is there an allochthonous 'Kerogen-2' in the rocks that had already lost its generative capacity due to higher maturity or reduced reactivity prior to entering this particular sediment? The compositional heterogeneity of kerogen was demonstrated by Williford et al. (2016), who observed micro-scale kerogen domains with strongly differing stable carbon isotopic composition in the ~2.8 Ga Tumbiana Formation. Such differences are difficult to explain, except by the presence of kerogen particles derived from different dominant metabolisms. This scenario is the most parsimonious way to explain all observations (see Section 4.5).

4.5 Compositional heterogeneity and different biological sources of alkanes

Predictably, the bulk saturated hydrocarbon fingerprint at Enspel changes with increasing thermal maturation. Our initial focus on the ULTRA fraction revealed that the most immature sample (Level 14) is strongly dominated by *n*-alkanes in the C_{25}–C_{31} range with an odd-over-even preference (OEP) and heptacosane as the dominant component (Fig. 6): a signature typical of vascular plant leaf waxes. This signature becomes diluted by unimodal-distributed *n*-alkanes (C_{23}–C_{37}, maximum at C_{29}) where the kerogen enters the oil window in Level 8, and has largely disappeared by Level 4 (note that a negligibly small OEP of 1.2 remains even in Level-2). The decrease in total bitumen yield above Levels 6 and 8 might be attributed to destructive cracking as a result of elevated temperatures, which is commonly accompanied by a shift towards lighter compounds, generally shorter *n*-alkanes. Yet we observe the opposite: the alkane fingerprint of the most mature Level 2 is heavier (C_{23}–C_{39}, maximum at C_{31}) than that of underlying strata. Level 4 is an exception to the trend with a lighter

signature accompanied by a slight UCM, which we attribute to minute variations in the source facies. The key observation is that the alkane OEP is only present *before* the oil generative window, suggesting that it stems from vascular plant leaf wax components and/or from alkanes that were never integrated into the kerogen macromolecular structure. It also implies that the majority of fatty acids and related structures that have been covalently merged into the kerogen, regardless of mechanism, are derived from bacteria or algae rather than land plants—bacteria being more likely given the relatively high abundance of hopanoids and paucity of steroids in all samples.

The fact that deltaic or lacustrine oils are often characterized by an OEP in the C_{27}–C_{33} region implies that, during incipient petroleum generation, this terrestrial signature is not reset. But early-generated hydrocarbons from the studied Enspel kerogens lack any OEP (progressive dilution of OEP in Levels 8 and 6), which stands in contrast to freely extractable compounds that have not been incorporated into the kerogen network (Levels 12 and 14). Possible explanations for this observation include reactions during catagenesis or, possibly more likely, a diagenetic effect where bacterial biomass is preferentially incorporated into the kerogen. The epicuticular wax fingerprint of different leaf species varies in the Miocene Clarkia Formation, and these waxes have not diffused from their fossil leaf fragments into the surrounding sediment (Logan et al., 1995). The same should be true both for macroscopic leaf fossils, as studied by Logan et al. (1995), and for microscopic leaf fragments. Either way, the immobility of waxes is congruent with our Enspel results and suggests that such waxes enter the sediment as free molecules associated with plant material. In the Enspel deposits, they were not (or only marginally) incorporated into the kerogen, which seems to represents an amalgam of products of largely bacterial and algal origin. In addition we observe that neither mature nor immature B2 samples contain any OEP land plant signal (Fig. 6). B2 in the least mature sample exhibits a unimodal alkane distribution around *n*-C_{22} (C_{17}–C_{31})—a pattern that persists relatively unchanged throughout the oil generative window (i.e. Levels 6 and 8), although the lighter alkanes become a little more prominent in these levels. In Level 2, the unimodal alkane fingerprint is shifted towards heavier compounds with *n*-C_{27} as the largest peak, similar to the trend observed in the ULTRA bitumens. The B2 composition at Level 4 appears to be a mixture between Level 2 and Level 6: a

bimodal alkane fingerprint exhibits maxima at *n*-C_{23} and *n*-C_{31}. The relatively uniform B2 alkane signature, in combination with the decrease in extract yield with increasing maturity, indicates that—similar to the waxes in the ULTRA extracts—this bitumen phase was already present as free hydrocarbons within the least mature sediment. In contrast to the waxes in ULTRA extracts, the B2 hydrocarbons did not become diluted by hydrocarbons generated from the co-occurring kerogen, as is evident from Level 6 upwards. This implies that B2 is shielded in some way and is not just an artifact of incomplete extraction.

The variation in the alkanes generated by the kerogen suggests that the Enspel sediment received organic input from at least three different pools: (i) primarily bacterial/algal kerogen (macromolecularly bound molecules) that released bitumen (i.e. free low molecular weight molecules) upon thermal maturation, (ii) free plant waxes that entered the sediment via plant fragments but which were not incorporated into the kerogen, and (iii) free, possibly-bacterial hydrocarbons (B2) that entered the sediment through an unknown route, but have not mixed with either of the first two phases or their released hydrocarbons.

4.6 Molecular indicators of source and facies

Immature ULTRA fractions (Levels 12 and 14) show a slight preponderance of C_{29} steranes (>50 %), diagenetic products of phytosterols characteristic of terrestrial sedimentary depocenters (Huang and Meinschein, 1979). Once the oil generative window is reached, the relative C_{29} abundance decreases with an increase in ergostane (Fig. 8b), suggesting that the latter is more abundant in the kerogen (the same overall trend is evident in the ASE extracts). Yet these trends are very subtle: no major difference in sterane homologs is evident between the ULTRA, ASE and B2 extracts, with the exception of B2 in Level 12, which exhibits an anomalously high abundance of C_{28} steranes that may reflect a subtle organofacies shift. Overall the consistent sterane distributions add confidence to the premise that the studied deposits reflect a highly uniform and stable organofacies in terms of summed biological input. The ratio of pristane to phytane (an indicator of depositional redox conditions: Didyk et al., 1978) fluctuates mildly, possibly with a slightly decreasing trend against thermal maturity in ULTRA and B2 extracts. This is contrary to observations of increasing

Pr/Ph values with thermal maturation (Connan, 1974; ten Haven et al., 1987), but is echoed by a decrease in such values in increasingly mature pyrolysates from the Green River Formation (Burnham et al., 1982). The Pr/Ph ratio is systematically lower in B2 than in ULTRA extracts (Fig. 11). The ASE values are slightly erratic, perhaps reflecting a low residual yield of these analytes. Despite the offset of 0.25–0.56, the variability in the Pr/Ph ratio is synchronized between ULTRA and B2 extracts, suggesting a common fluctuation of depositional redox and excluding the possibility that B2 originated from a different depositional setting, e.g. as a terrigenous detrital phase with adsorbed allochthonous organic matter.

4.7 Mineralogical clues to the locale of Bitumen 2

Given that B2 cannot be recovered without digesting the mineral matrix, a true physical occlusion has frequently been assumed, evoking the idea that B2 resides in fluid inclusions within individual secondary-growth minerals or healed-and-sealed fractures. However, B2 also occurs as a phase, chemically distinct from free bitumen, where the abundance and quality of organic matter is insufficient to expel discrete hydrocarbon fluid phases (e.g. Nabbefeld et al., 2010), and a link between B2 and fluid inclusions has never been established. The alternative hypotheses are that B2 is closely associated with either a specific kerogen pool or with clay minerals. The observation that B2 does not increase in abundance across the oil generative window (in contrast to the ULTRA and ASE bitumens) indicates that it could be derived from an inert or 'spent' kerogen, possibly of detrital origin, if it is associated with macromolecular organic matter. Compositional heterogeneity is known in kerogens (Williford et al., 2016) and might be attributed to mixing of an allochthonous black carbon phase with biomass produced in the water column. However there is no obvious mechanism that would lead to a B2 phase that is spatially segregated from kerogen formed from primary organic matter and its derivative bitumen.

What is more likely is that B2 comprises clay-adsorbed hydrocarbons that are transported on detritus entering the sedimentary environment. Acidic sites on clay minerals can catalyze rearrangements within molecules, including the formation of diasteranes (Rubinstein et al., 1975; Sieskind et al., 1979; Peakman and Maxwell, 1988; Peakman et al., 1988) and diahopanes (e.g. Moldowan et al., 1991). The degree

of rearrangement is influenced by the clay/TOC ratio (that is, available clay sites) rather than clay mineral abundances, and clay minerals also influence thermal maturity parameters based on stereoisomerization (Van Kaam-Peters et al., 1998). While the Enspel samples yielded no diahopanes, the relative abundance of dia- over regular steranes in B2 was consistently elevated over ULTRA and ASE fractions—the dia-/regular sterane ratio is very similar in both, apart from the most mature sample (Fig. 11; an exception is Level 8, where the dia/regular ratio of B2 matches that of free bitumen). The greater rearrangement of steranes in B2 supports the hypothesis that B2 is partially or largely adsorbed to the clay fraction and has experienced more extensive catalysis. Yet what remains inconsistent with this hypothesis is the co-variation of Pr/Ph ratios in free (ULTRA) and B2 fractions (Section 4.6), which suggests derivation from an environment with the same fluctuation of depositional redox conditions.

Irreversible adsorption of both hydrocarbons and asphaltenes on sediments (e.g. Kan et al., 1994; Berkowitz et al., 2014) is primarily driven by sorptive interaction with clays (Dubey and Waxman, 1991). Such a process may explain the nature of Enspel B2: adsorbed components are not susceptible to solvent extraction until the clay minerals have been digested. The absence of plant derived OEP alkanes (Section 4.5) might be interpreted as evidence that Enspel B2 is protected, while plant waxes are tightly associated with their source phytoclasts and may be unavailable.

There is a degree of compositional overlap between free bitumen and B2, revealed by later ASE fractions. Nevertheless, it is evident that B2 represents a hydrocarbon phase (i.e. one not bound within a macromolecular network) that is tightly adsorbed onto clay minerals, or onto carbon phases protected by, and tightly associated with clay minerals. The previously mentioned co-varying Pr/Ph trends do not support a completely allochthonous source of compounds (such as soils or older weathered rocks). It is however possible that the clay minerals record a cumulative molecular snapshot starting in the upper water column. Phytol mostly degrades to pristane in oxygenated waters (Wakeham, 1990). Sediments primarily record the residue of the pristane and phytane produced from more rapidly sinking organic matter below the oxycline. The inventory of clay-adsorbed hydrocarbons may reflect an enhanced upper-water column signature due to sorptive protection (Keil et al., 1994), which

would explain higher Pr/Ph values in B2, yet a covariation with ULTRA and ASE. Bovee and Pearson (2014) showed that the biomarker signature of pelagic photosynthetic sulfur bacteria in meromictic Lake Mahoney is not preserved: the lake bottom carries a shoreline signature, possibly due to rapid transport of mineral ballasted littoral organic matter. Likewise clay-associated hydrocarbons in the Enspel samples may preserve a littoral or upper water column molecular signature, and become transported together with clay minerals and/or refractory organic matter. Such considerations suggest that a stronger emphasis on molecular taphonomy and its relationship with mineralogy might result in a better understanding of otherwise inconsistent geochemical data.

4.8 Thermal maturation observed at the molecular level

Our study reveals a discrepancy between the expected response of various molecular proxies to thermal maturation and physically observed changes in the layers below the lava flow (Section 4.1). Rock Eval maturity data and palynological organic matter color appear too high relative to vitrinite reflectance values, although these are difficult to determine with confidence (Sections 3.1.3 and 3.1.4), and the preservation of diagnostic polycyclic terpenoid hydrocarbons is unexpected. This mismatch continues on a molecular level. Thermal cracking of hydrocarbons should be an important mechanism at such thermal maturities but the average chain length in all bitumen fractions increases towards the lava flow (Figs. 6, 11), presumably reflecting generation of slightly heavier components.

4.8.1 Trisnorhopanes: Ts, Tm and Tb

The relative abundance of Ts over Tm typically increases with thermal maturation as a consequence of the lower thermal stability of the latter (Seifert and Moldowan, 1978). If elevated temperature is excluded as a cause of molecular cracking and destruction (Section 3.2.2), it is surprising that the Ts/(Ts+Tm) ratio changes at all in the Enspel samples (Fig. 7), although it only increases in Levels 2 and 4 closest to the lava flow (Fig. 12). But contrary to expectation, Level 2 yields a lower value than Level 4. A similar observation was presented by Farrimond et al. (1998) who observed a rapid increase of Ts/(Ts+Tm) around 436–444ºC T_{MAX}, followed by a

renewed drop above ~456ºC, and decreasing values of % Ts have been previously reported around igneous intrusions (Farrimond et al., 1996). This may imply that the rearranged hopane structure is not present in kerogens as such, but is formed during the release of regular hopanoids under specific conditions (Farrimond et al., 1998).

The Ts/(Ts+Tm) parameter is generally suppressed in pure carbonate lithologies and elevated in shales (e.g. McKirdy et al., 1983, 1984; strongly elevated values in hypersaline settings—e.g. Rullkötter and Marzi, 1988—are likely due to the evaporative concentration of metals and their catalytic potential after complexation into kerogen), which suggests sensitivity to clay catalyzed reactions (Peters and Moldowan, 1993). A systematic relative elevation of diasteranes occurs in B2 in the Enspel samples and a similar, but less pronounced, trend is evident in Ts/(Ts+Tm). The greater similarity between ASE and B2 extracts *vs.* ULTRA extracts (Fig. 12) suggests that a compositional gradient is obtained during sequential extractions, and that B2 is actually not completely shielded. In the Enspel sequence 22,29,30-trisnor-17β(H)-hopane (henceforth termed Tb) is much more prominent than either Ts or Tm in the least mature samples (Fig. 7). Tb has been reported to disappear at the onset of the oil window, paralleled by an increase in Ts (Hong et al., 1986). Based on increased bitumen/TOC ratios, the Enspel sequence is thought to traverse the oil window in Levels 6 and 8. While Tb appears to be progressively converted to Tm—not Ts—it is still present in the most mature samples. Thus the Ts/(Ts+Tm) maturity parameter is not a reliable indicator of thermal maturity below the oil generative window. The ratio (Ts+Tm)/(Ts+Tm+Tb), which shows a gradual increase in the Enspel sequence (Fig. 12), is more applicable in this case.

In the least mature Level 14 a similarly high Tb (i.e. 17β) peak is evident in both free and occluded bitumens (Fig. 7), yet its conversion proceeds differently. Tb is mainly converted to Tm with consistently low Ts levels in free bitumens, whereas B2 exhibits a more pronounced increase of Ts, rather than Tm, from Level 6 upwards. We attribute this differential evolution to the catalytic influence of clay minerals, as observed for diasteranes. The relative abundance of Ts over Tm, or over Tm+Tb, reflects not only the effects of thermal maturation, but also of catalytic conversion, and confirms the potential utility of the ratio (Ts+Tm)/(Ts+Tm+Tb) below the oil generative window.

4.8.2 The relative abundance of C_{29}, C_{30} and C_{31} hopanes

Both C_{29} and C_{30} hopanoids are thought to derive from C_{35}+ bacteriohopanepolyols, and elevated C_{29}/C_{30} ratios are often indicative of carbonate lithologies (Fan Pu et al., 1988; ten Haven et al., 1988; Subroto et al., 1991, 1992). The Enspel samples show a slight but systematic elevation of C_{29} over C_{30} hopanoids in B2, and the opposite signature in free bitumens (Fig. 7). This signature is evident in the ββ-hopanes in the least matured sample and throughout the sequence; it is also paralleled in an increase in βα and αβ-hopanes with increasing thermal maturity due to the conversion of ββ-hopanes. This observation cannot be directly related to elevated C_{29}/C_{30} hopane ratios in carbonate source lithologies since the Enspel sequence is particularly poor in carbonate. In contrast to the observed increase in clay-catalyzed rearrangement of molecules in B2 with thermal maturity, the C_{29}/C_{30} pattern and offsets remain relatively constant throughout the maturity sequence: the ratio is neither maturity driven, nor a response to clay catalysis. The discrepancy between hopanoids in free and occluded bitumen is evident in the pattern of ββ-hopanes; their differential signature suggests a slightly different biological input, perhaps including the proportion of hexasubstituted bacteriohopanepolyols, which are bound onto clays harboring the B2. Apart from the differences in the C_{29}/C_{30} pattern between free and occluded bitumen, the free bitumen fractions contain a larger relative abundance of C_{31} ββ-hopanes in the least mature sample. This larger abundance appears to disappear with increasing thermal maturity and is neither maintained in remnant ββ-hopanes in thermally more mature samples, nor transferred to βα or αβ-hopanes. It is possible that C_{31} is converted to smaller hopanes with increased thermal maturation of free bitumen, but the absence of a similar decline in C_{31} hopanes in B2 argues against such a process and leaves this observation unexplained.

4.8.3 Hopanoid and steroid stereochemistry

The ββ hopanes are progressively replaced by βα and αβ-hopanes (Fig. 8A) but to a different degree and with different kinetics for B1 and B2. The latter contains significantly more ββ-hopanes than ULTRA extracts in immature levels, while ASE

extracts appear to represent an intermediate state. The relative abundance of αβ-hopanes, however, is similar and thus B1 (ULTRA) contains a significant higher proportion of moretanes. Positive moretane anomalies have been attributed to increased input of soil organic matter with detrital clays (French et al. 2012) but this does not apply at Enspel as the probably-clay-bound B2 is characterized by relatively lower moretane abundances. Moretanes are most abundant in immature ULTRA extracts but remain abundant even in those ULTRA samples that have experienced the highest thermal overprint. Amongst the most mature samples, ASE and B2 extracts have accumulated more thermally converted αβ-hopanes than the free bitumen ULTRA extracts. Our data suggest that no newly generated bitumen contributed to the B2 pool (Section 4.7). It is thus likely that ULTRA extracts experience not only a conversion of hopanes that are present as free hydrocarbons prior to entering the oil generative window, but also the release of hopanes from the kerogen. If these newly generated hopanes have elevated βα/αβ ratios, in line with a terrigenous-lacustrine origin of the kerogen (e.g. Isaksen and Bohacs, 1995), the observed discrepancies could be explained by a combination of conversion and generation.

ASE extracts of immature samples are more similar to ULTRA extracts than to B2 extracts, but once samples enter the oil generative window, the ASE extracts take on an increasingly B2-like signature. For both C_{29} and C_{30} hopanes, the βα/(αβ+βα) index is observed to decrease with thermal maturation (Fig. 12) (Seifert and Moldowan, 1980). However, it is clear that the B1 fractions (i.e. ULTRA and ASE) share the same maturity values at stratigraphic levels below the oil window (i.e. below Levels 6 and 8), whereas B2 fractions show different values. Once the oil window is entered, all values converge and beyond this, the free ASE and occluded B2 share the same thermal maturity values, whereas those for the free ULTRA bitumen differ. A similar pattern is also evident for the 22*S*/(22*S*+22*R*) ratio in C_{31} homohopanes. In the case of the βα/(αβ+βα) parameter it appears that ULTRA and ASE respond to thermal maturation below Level 6, whereas B2 remains relatively constant. ASE bitumen continues to mature stratigraphically above Level 6, and is joined by B2 hopanes that begin to respond to the temperature increase, while ULTRA remains relatively constant. We hypothesize that from Level 6 stratigraphically upwards, the ULTRA fraction becomes mixed with less mature bitumen that has migrated upwards. Hence,

maturity between Levels 14 and 6 is indicated by both ULTRA and ASE (in these levels B2 appears more mature), whereas above Level 6 maturity is recorded in ASE and B2. ULTRA would presumably also show this latter trend above Level 6 if it had not received an admixing phase of less mature bitumen that probably originates around Level 6. Our data show that B2 is not affected by migrating oil in contrast to ASE, again indicating that B2 is shielded to some degree. An outstanding question is why the composition of B2 appears largely consistent until Level 6 and only reacts to thermal maturation at higher levels. B2 below Level 6 appears to be matured already. The proportions of ββ, βα and αβ-hopanes are already at a level where initial temperature increases do not affect the relative composition. Hopanoid ratios indicate that below Level 6 B2 is at a relatively constant level of thermal maturation, which could be due either to catalysis-enhanced isomerization, or to a source of pre-matured B2 hopanoids. The pattern for C_{30} and C_{29} hopanes is identical except that below Level 6, B2 is *less* instead of more mature, although the offset in βα/(αβ+βα) to ASE and ULTRA is minimal here. Clay minerals entering the depositional environment may have already entrained a hopanoid suite of adsorbed hydrocarbons that was strongly enriched in C_{30} hopanes (for a similar scenario, see data in Sepùlveda et al. 2009).

The Enspel data suggest that B2 is not an artifact of incomplete extraction but a distinct phase that can be mixed to some degree with free bitumen. A continuous change in molecular composition throughout the sequential extraction applied in this study is evidenced by progressive changes in the average chain length (ACL) of bitumens, as well as their carbon number preference (CPI-1): a continuous trend is evident from ULTRA via ASE-1 to ASE-6 and B2 (Fig. 11). This testifies to the spatial and compositional inhomogeneity of bitumens in these rocks.

While steroid-based maturity parameters in all bitumens throughout the Enspel sequence appear either invariant or slightly erratic, a striking pattern is observed in the 20*S*/(20*S*+20*R*) parameter determined separately for C_{27}, C_{28} and C_{29} steranes (Fig. 13). The value of this parameter in B2 increases gradually with thermal maturation, but the values between sterane isomers are offset: C_{27} is the most mature and C_{29} the least. This pattern is neither observed in free bitumen, nor in the 14,17-ββ/(ββ+αα) ratios. Locally produced biomass may have been enriched in C_{29} steranes, while

detrital clays introduced steranes dominated by C_{27} that had already undergone thermal maturation. In this case 20*S*/20*S*+20*R* may be more sensitive to initial thermal maturation than ββ/(ββ+αα) (Peters et al., 2005).

The values we obtained for the various molecular maturity parameters in the Enspel samples reveal significant differences in the stage of thermal maturity they indicate (Fig. 10). Clearly, rapid high temperature maturation of organic matter can lead to results that are complicated to interpret within the traditional framework of progressive thermal maturation in a slowly subsiding basin.

5. CONCLUSIONS

Our data show that the composition and yield of extracted bitumen from the Enspel Formation is strongly dependent on the extraction technique and the maturity of the organic matter: immature samples tend to release a larger proportion of their bitumen during gentle extraction by ultrasonic agitation, and more mature samples require more vigorous solvent extraction. Hence comparing the results of different extraction techniques, or of ultrasonic extracted bitumens of differential maturity, could lead to erroneous conclusions. During sequential extraction, polycyclic terpenoids were more readily extracted than *n*-alkanes. Sequential extraction also revealed a gradual and systematic shift towards shorter average chain lengths, the loss of carbon number preference (where present in immature samples), and greater stereochemical rearrangement (potentially indicative of elevated maturity). Occluded B2, recovered after mineral digestion, revealed a higher thermal maturity, systematically higher Pr/Ph values, and completely different alkane fingerprints, confirming that B2 represents a separate phase, which experienced minimal mixing with the free bitumen that is readily extractable prior to mineral digestion. B2 also contained abundant diasteranes, which were nearly absent in extracts recovered prior to digestion, suggesting enhanced catalysis and a tight association of B2 with clay minerals or kerogen. This observation suggests that B2 can in certain cases be protected against contamination and therefore represents a valuable reservoir of indigenous biomarker information. Nevertheless, if the higher maturities in B2 are caused by intrinsic mechanistic effects, it may also be subject to faster degradation by cracking.

Although our data did not allow us to establish the precise origin of the hydrocarbons in B2, we rather tend to exclude a completely different environment on the basis of systematic co-variation of the Pr/Ph redox parameter in all studied bitumen phases. We propose that free hydrocarbons, which are irreversibly bound to clay minerals during early diagenesis, represent a mixture of 'fresh' components derived from primary production and reworked hydrocarbons. Our data also suggest that different phases—older, younger and maybe detrital—within B2 are adsorbed on different clay minerals, and confirm that B2 is not an artifact of incomplete extraction. The results of the Enspel study highlight the spatial and compositional heterogeneity of bitumen that has hitherto escaped systematic attention, and which could allow an enhanced understanding of organic matter pools and sources when studied more systematically. The recognition of a distinct B2 phase highlights its potential as a source of new information from Precambrian samples which may provide more insights into the nature of the early biosphere.

Elaborate biomarker studies benefit from prior screening of hydrocarbon preservation potential with indicators such as the H/C ratio of their host kerogens or the color of co-occurring organic matter or vitrinite reflectance values. Previous calibrations have set a cutoff at spore color index (SCI) values of ~8–9, corresponding roughly to the upper oil window, or at T_{max} values around 440ºC. The sedimentary sequence of Lake Enspel experienced rapid thermal alteration at elevated temperatures resulting in discordant maturity indicators: despite brown to black palynological organic matter coloration (colors 8–10) and T_{max} values between ca. 430º and 520ºC, the measured vitrinite reflectance (albeit based on few samples) does not exceed 1.1 %, bitumens appear only marginally mature, and biomarkers are well preserved. Such circumstances demand calibration based on multiple indicators of thermal maturity, as such parameters appear strongly dependent on the time–pressure-temperature pathway of organic matter maturation.

ACKNOWLEDGEMENTS

Rich D. Pancost and Neal Gupta are thanked for their constructive comments and contributions during the earliest stages of the project. Michael Wuttke and Marcus Poschmann provided access and assistance at the Enspel site. We thank Sharon Newman and Carolyn Colonero for laboratory support and Julio Sepulveda for useful discussions. At Royal Holloway University of London, Neil Holloway is thanked for the production of the polished blocks and thin sections and Sharon Gibbons for preparing the palynological organic matter slides. Youssef Espidel and Muriel Rakotomalala assisted with analyses during early stages of the project. CJI was funded through DFG grant STR 281/32 to HS. CH was supported by the Agouron Institute and by the Max Planck Society. RES and DEGB were supported by the NASA Astrobiology Institute (NNA13AA90A) Foundations of Complex Life, Evolution, Preservation, and Detection on Earth and Beyond.

REFERENCES

Arouri K. R., Al-Saleh S. H. and Al-Hilal Z. M. (2009) Residual oil as a tool in migration and filling history analysis of petroleum reservoirs, Ghazal Field, Saudi Arabia. *Org. Geochem.* **40**, 617–627.

Behar F. and Vandenbroucke M. (1988) Characterization and quantification of saturates trapped inside kerogen: Implications for pyrolysate composition. *Org. Geochem.* **13**, 927–938.

Bennett B. and Abbott G. D. (1999) A natural pyrolysis experiment – hopanes from hopanoic acids? *Org. Geochem.* **30**, 1509-1516.

Berkowitz B., Dror I. and Yaron B. (2014) Contaminant Geochemistry. Springer-Verlag, Berlin Heidelberg, 577 pp.

Bishop A. N. and Abbott G. D. (1993) The interrelationship of biological marker maturity parameters and molecular yields during contact metamorphism. *Geochim. Cosmochim. Acta* **57**, 3661-3668.

Bovee R. J. and Pearson A. (2014) Strong influence of the littoral zone on sedimentary lipid biomarkers in a meromictic lake. *Geobiology* **12**, 529-541.

Bray E. E. and Evans E. D. (1961) Distribution of n-paraffins as a clue to recognition of source beds. *Geochim. Cosmochim. Acta* **22**, 2-15.

Briggs D. E. G. (1999) Molecular taphonomy of animal and plant cuticles: selective preservation and diagenesis. *Phil. Trans. R. Soc. London B: Biological Sciences* **354**, 7-17.

Brocks J. J., Grosjean E. and Logan G. A. (2008) Assessing biomarker syngeneity using branched alkanes with quarternary carbon (BAQCs) and other plastic contaminants. *Geochim. Cosmochim. Acta* **72**, 871-888.

Brocks J. J. (2011) Millimeter-scale concentration gradients of hydrocarbons in Archean Shales: Live-oil ecape or fingerprint for contamination. *Geochim. Cosmochim. Acta* **75**, 3196-3213.

Burnham A. K., Clarkson J. E. Singleton M. F., Wong C. M. and Crawford R. W. (1982) Biological markers from Green River kerogen decomposition. *Geochim. Cosmochim. Acta* **46**, 1243-1251.

Clausing A. (1998) Mikro-organofazielle Studien an Sedimenten des Enspel-Sees (Oberoligozän, Westerwald, Deutschland). *Hallesches Jahrb. Geowiss.* **B20**, 119–133.

Cody G. D., Gupta N. S., Briggs D. E. G., Kilcoyne A. L. D., Summons R. E., Kenig F., Plotnick R. E. and Scott A. C. (2011) Molecular signature of chitin-protein complex in Paleozoic arthropods. *Geology* **39**, 255-258.

Collins A. (1990) The 1–10 Spore Colour Index (SCI) scale: a universally applicable colour maturation scale, based on graded, picked palynomorphs. *Mededelingen Rijks Geologische Dienst* **45**, 39–47.

Collinson M. E. (2011) Molecular taphonomy of plant organic skeletons. In *Taphonomy, Second Edition: Process and Bias Through Time* (eds. P. A. Allison and D. J. Bottjer), *Topics in Geobiology* **32**, Springer Science+Business Media B.V. DOI 10.1007/978-90-481-8643-3_6,

Connan J. (1974) Diagenese naturelle et diagenese artificielle de la matière organique à element vegetaux predominanntes. In: *Advances in Organic Geochemistry* (eds. B.P. Tissot and F. Bienner) Technip, Paris, pp. 73-95.

Didyk B. M., Simoneit B. R. T., Brassell S. C. and Eglington G. (1978) Organic geochemical indicators of paleoenvironmental conditions of sedimentation. *Nature* **272**, 216-222.

Dubey S. T. and Waxman M. H. (1991) Asphaltene adsorption and desorption from mineral surfaces. *SPE Reservoir Engineering* **18462**, 389–395.

Durand B. (1980) Sedimentary organic matter and kerogen. Definition and quantitative importance of kerogen. In: *Kerogen, Insoluble Organic Matter from Sedimentary Rocks* (Ed. Durand, B.). Editions Technip, Paris, 13–34.

Eigenbrode J. L. (2004) Late Archean microbial ecology: An integration of molecular, isotopic and lithologic studies. PhD Thesis. The Pennsylvania State University.

Espitalié J., Laporte J. L., Madec M., Marquis F., Leplat P., Paulet J. and Boutefeu A. (1977) Rapid method for source rock characterization, and for determination of their petroleum potential and degree of evolution. *Rev. Inst. Franc. Petr. Ann. Combust. Liq.* **32**, 23-42.

Fan Pu, King J. D. and Claypool G. E. (1988) Characteristics of biomarker compounds in Chinese crude oils. In:, *Proceedings of the first International Conference on Petroleum Geochemistry and Exploration in the Afro-Asian Region, Dehradun, 25-27 November 1985: Rotterdam, Balkema* (eds. R. K. Kumar, P. Dwivedi, V. Banerjie, and V. Gubta),pp. 197-202.

Farrimond, P., Bevan, J. C. and Bishop, A. N. (1996) Hopanoid hydrocarbon maturation by an igneous intrusion. *Org. Geochem.* **25**, 149–164.

Farrimond P., Taylor A., TelnÆs N. (1998) Biomarker maturity parameters: the role of generation and thermal degradation. *Org. Geochem.* **29,** 1181–1197.

Ferralis N. Matys E. D., Knoll A. H., Hallmann C. and Summons R.E., (2016) Rapid, direct and non-destructive assessment of fossil organic matter via microRaman spectroscopy. *Carbon* **108**, 440 - 449.

Fisher M. J., Barnard P. C., and Cooper B. S. (1980) Organic maturation and hydrocarbon generation in the Mesozoic sediments of the Sverdrup basin, Arctic Canada. *Fourth International Palynological Conference, Lucknow, India, Proceedings* **2**, 581-588.

French K. L., Tosca N. J., Cao C. and Summons R. E. (2012) Diagenetic and detrital origin of moretane anomalies through the Permian-Triassic boundary. *Geochim. Cosmochim. Acta* **84**, 104-125.

French K., Hallmann C., Hope J., Schoon P. L., Zumberge J. A., Hoshino Y., Peters C. A., George S. C., Love G. D., Brocks J. J., Buick R., and Summons R. E. (2015) Reappraisal of hydrocarbon biomarkers in Archean rocks. *Proc. Nat. Acad. Sci.* **112**, 5915–5920.

Gaupp R. and Wilke A., (1998) Zur Sedimentologie der oberoligozänen Seesedimente von Enspel/Westerwald. *Hallesches Jahrb. Geowiss.* **B20**, 97–118.

Grosjean E., Love G. D., Stalvies C., Fike D.A. and Summons R.E. (2009) Origin of petroleum in the Neoproterozoic-Cambrian South Oman Salt Basin. *Org. Geochem.* **40**, 87–110.

Gupta N. S., Briggs D. E. G., Collinson M. E., Evershed R. P., Michels R., and Pancost, R. D. (2007) Molecular preservation of plant and insect cuticles from the Oligocene Enspel Formation, Germany: Evidence against derivation of aliphatic polymer from sediment. *Org. Geochem.* **38**, 404-418.

Gupta N. S., Cody G. D., Tetlie O. E., Briggs D. E. G. and Summons R. E. (2009) Rapid incorporation of lipids into macromolecules during experimental decay of invertebrates: Initiation of geopolymer formation. *Org. Geochem.* **40**, 589-594.

Hallmann C. O. E., Arouri K. R., McKirdy D. M. and Schwark L. (2006) A new perspective on exploring the Cooper/Eromanga petroleum province - Evidence of oil charging from the Warburton Basin. *APEA Journ.* **46**, 261–282.

Hallmann C. O. E., Arouri K. R., McKirdy D. M. and Schwark L. (2007) Temporal resolution of an oil charging history – A case study of residual oil benzocarbazoles from the Gidgealpa Field. *Org. Geochem.* **38**, 1516-1536.

Hallmann C., Kelly A. E., Gupta N. S. and Summons, R. E. (2011) Reconstructing deep-time biology with molecular fossils. In *Quantifying the evolution of early life. Topics in Geobiology*, **36** (eds. M. Laflamme, J. D. Schiffbauer and S. Q. Dornbos) Springer. Pp. 355–401.

Harris N. B. and Peters, K. E. (2012) Analyzing thermal history of sedimentary basins: Methods and case studies-Introduction. In *Analyzing thermal history of sedimentary basins: Methods and case studies. SEPM Special Publication* **103** (eds. N.B. Harris and K.E. Peters), pp. 1-4.

Hartkopf-Fröder C., Königshof P., Littke R. and Schwarzbauer J. (2015) Optical thermal maturity parameters and organic geochemical alteration at low grade diagenesis to anchimetamorphism: a review. *Int J Coal Geol* **150-151**, 74-119.

Herrmann M. (2007) Eine palynologische Analyse der Bohrung Enspel. Rekonstruktion der Klima- und Vegetationsgeschichte im Oberoligozän. PhD Thesis, Eberhard-Karls-Universitaet Tuebingen. 253 pp.

Herrmann M. (2010) Palaeoecological reconstruction of the late Oligocene Maar Lake of Enspel, Germany using lacustrine organic walled algae. *Palaeobiodiversity and palaeoenvironments* **90**, 29-37.

Holman A. I., Grice K., Jaraula C. M. B., Schimmelmann A. and Brocks J. J. (2012) Efficiency of extraction of polycyclic aromatic hydrocarbons from the Paleoproterozoic *Here's Your Chance* Pb/Zn/Ag ore deposit and implications for a study of Bitumen II. *Org. Geochem.* **52**, 81–87.

Holman A. I., Grice K., Jaraula C. M. B. and Schimmelmann A. (2014) Bitumen II from the Paleoproterozoic *Here's Your Chance* Pb/Zn/Ag deposit: Implications for the analysis of depositionalenvironmenzt and thermal maturity of hydrothermally-altered sediments. *Geochim. Cosmochim. Acta* **139**, 98-109.

Hong Z.-H., Hui-Ziang L., Rullkötter J. and Mackenzie A.S. (1986) Geochemical application of steranes and triterpane biological marker compounds in the Linyi Basin. *Org. Geochem.* **10**, 433-439.

Horn P. and Müller-Sohnius D. (1988) A differential etching and magnetic separation approach to whole-rock potassium-argon dating of basaltic rocks. *Geochem. J.* **22**, 115-128.

Huang W.-J. and Meinschein W.G. (1979) Sterols as ecological markers. *Geochim. Cosmochim. Acta* **43**, 739-745.

Illing C. J., Hallmann C., Miller K. E., Summons R. E. and Strauss H. (2014) Airborne hydrocarbon contamination from laboratory atmospheres. *Org. Geochem.* **76**, 26-38.

Isaksen G. H. and Bohacs K. M. (1995) Geological controls on source rock geochemistry through relative sea level; Triassic, Barents Sea. In *Petroleum Source Rocks* (ed. B. J. Katz),Springer-Verlag, New York, pp. 25-50.

Jarvie D M., Morelos A. and Han Z. (2001) Detection of pay zones and pay quality, Gulf of Mexico: Application of geochemical techniques: Gulf Coast Association of Geological Societies Transactions **51**, pp. 151-160.

Kan A. T., Fu G. and Tomson M. B. (1994) Adsorption/desorption hysteresis in organic pollutant and soil/sediment interaction. *Environmental Science & Technology* **28**, 859-867.

Keil R. G., Montlucon D. B., Prahl F. G. and Hedges J. I. (1994) Sorptive preservation of labile organic matter in marine sediments. *Nature* **370**, 549-552.

Killops S. D. and Killops V. J. (2005) Introduction to Organic Geochemistry. Wiley-Blackwell, 408 pp.

Köhler J. (1998) Die Fossillagerstätte Enspel—Vegetation, Vegetationsdynamik und Klima im Oberoligozän. PhD Thesis. University of Tübingen, Tübingen.

Kramer L., McKirdy D. M., Arouri K. R., Schwark L. and Leythaeuser D. (2004) Constraints on the hydrocarbon charge history of sandstone reservoirs in the Strzelecki Field, Eromanga Basin, South Australia. *Proceedings of the PESA Eastern Australian Basin Symposium II*, pp. 589-602.

Kuila U., McCarty D. K., Derkowski, A., Fischer, T. B., Topór T. and Prasad, M. (2014) Nano-scale texture and porosity of organic matter and clay minerals in organic-rich mudrocks. *Fuel* **135**, 359-373.

Lafargue E., Marquis F. and Pillot D. (1998) Rock-Eval 6 applications in hydrocarbon exploration, production and soil contamination studies. *Rev. Inst. Franc. Petr. Ann. Combust. Liq.* **53**, 421-437.

Larter S. R. and Aplin A. C. (1995) Reservoir geochemistry: methods, application and opportunities. In *The geochemistry of reservoirs. Geological Society Special Publication* **86 (**J. M. Cubitt and W. A. England eds.) pp. 5–32.

de Leeuw J., Versteegh G. and van Bergen P. (2006) Biomacromolecules of algae and plants and their fossil analogues. *Plant Ecol.* **182**, 209–233.

Leider, A., Schumacher, T.C., Hallmann, C., 2016. Enhanced procedural blank control for organic geochemical studies of critical sample material. *Geobiology* **14**, 469–482.

Leythaeuser D., Keuser Ch. and Schwark L. (2007). Molecular memory effects recording the accumulation history of petroleum resrevoirs: The Heidrun Field, offshore Norway, as an example. *Marine and Petroleum Geology* **24**, 199-220.

Leythaeuser D., Littke R., Radke M. and Schaefer R.G. (1988) Geochemical effects of petroleum migration and expulsion from Toarcian source rocks in the Hils syncline area, NW-Germany. *Org. Geochem.* **13**, 489-502.

Leythaeuser D., Poelchau H.S. (1991) Expulsion of petroleum from Type III kerogen source rocks in gaseous solution: modeling of solubility fractionation. In: Petroleum migration. *Geological Society Special Publication* **59 (**W.A. England, A.J. Fleet eds.). pp 33–46.

Littke R., Baker D. R. and Leythaeuser D. (1988) Microscopic and sedimentologic evidence for the generation and migration of hydrocarbons in Toarcian source rocks of different maturities. *Org. Geochem.* **13**, 549-559.

Löhr S. C., Baruch E. T., Hall P. A. and Kennedy M. J. (2015) Is organic pore development in gas shales influenced by the primary porosity and structure of thermally immature organic matter? *Org. Geochem.* **87**, 119-132.

Logan G. A., Smiley C. J. and Eglington G. (1995) Preservation of fossil leaf waxes in association with their source tissues, Clarkia, northern Idaho, USA. *Geochim. Cosmochim. Acta* **59**, 751-763.

Lüniger G. (2002) Chemofazies der oligozänen Schwarzpelite von Enspel (Westerwald, Rheinland-Pfalz). Dissertation, Univ. Köln.

Lüniger G. and Schwark L. (2002) Characterization of sedimentary matter by bulk and molecular geochemicall proxies: an example from Oligozän maar-type Lake Enspel, Germany. *Sed. Geol.* **148**, 275-288.

McKirdy D. M., Aldridge A. K. and Ympa P. J. M. (1983) A geochemical comparison of some crude oils from Pre-Ordovician carbonate rocks. In *Advances in Organic Geochemistry 1981* (eds. M. Bjoroy et al.) John Wiley & Sons, New York, pp. 99-107.

McKirdy D. M., Kantsler A. J., Emett J. K. and Aldridge A. K. (1984) Hydrocarbon genesis and organo facies. in Cambrian carbonates of the Eastern Officer Basin, South Australia. In *Petroleum Geochemistry and Source Rock Potential of carbonate rocks* (ed. J.G. Palacas), AAPG, Tulsa, pp.13-31.

Mertz D. F., Renne P. R., Wuttke M. and Mödden C. (2006) A numerically calibrated reference level (MP28) for the terrestrial mammal-based biozonation of the European Upper Oligocene. *Int. J. Earth Sci.* **96**, 353-361.

Mitchell R. H. (2001) Measuring aromaticity by NMR. *Chem. Rev.* **101**,1301–1315.

Modica C. J. and Lapierre S. G. (2012) Estimation of kerogen porosity in source rocks as a function of thermal transformation: Example from the Mowry Shale in Powder River Basin of Wyoming. *AAPG Bull.* **96**, 87-108.

Moldowan J. M., Fago F. J., Carlson R. M. K., Young D. C., an Duvne G., Clardy J., Schoell M., Pillinger C. T. and Watt D. S. (1991) Rearranged hopanes in sediments and petroleum. *Geochim. Cosmochim. Acta* **55**, 3333-3353.

Nabbefeld B., Grice K., Schimmelmann A., Summons R. E., Troitzsch U. and Twitchett R. J. (2010) A comparison of thermal maturity parameters between freely extracted hydrocarbons (Bitumen 1) and a second extract (Bitumen 2) from within the kerogen matrix of Permian and Triassic sedimentary rocks. *Org. Geochem.* **41**, 78-87.

Palciauskas V. V. (1991) Primary migration of petroleum. In *Source and migration processes and evaluation techniques* (Ed. R.K. Merrill). The American Association of Petroleum Geologists, Tulsa. pp.13-22.

Peakman T. M. and Maxwell J. R. (1988) Early diagenetic pathways of steroid alkenes. *Org. Geochem.* **13**, 583-592.

Peakman T. M., Ellis K. and Maxwell J. R. (1988) Acid-catalysed rearrangements of steroid alkenes. Part2. A re-investigation of the backbone rearrangement of cholest-5-ene. *Journal of Chemical Society, Perkin Transaction I*, 1071-1075.

Pepper A. S. (1991) Estimating the petroleum expulsion behaviour of source rocks: a novel quantitative approach. In: *Petroleum migration*. Special Publication **59** (Eds. W. A. England and A. J. Fleet). Geological Society, London. pp. 9–32.

Peters K. E. (1986) Guidelines for evaluating petroleum source rock using programmed pyrolysis. *AAPG Bull.* **70**, 318-329.

Peters K. E. and Moldowan J. M. (1993) The Biomarker Guide. Interpreting Molecular Fossils in Petroleum and Ancient Sediments. Prentice-Hall, Englewood Cliffs.

Peters K. E. and Cassa M. R. (1994) Applied source rock geochemistry. In: *The petroleum system-from source to trap*. AAPG Memoir **60**.

Peters K. E., Walters, C. C. and Moldowan J. M. (2005) The Biomarker Guide. Cambridge Univ. Press, New York, 1155 pp.

Petschick R., Kuhn G. and Gingele F. (1996) Clay mineral distribution in surface sediments of the South Atlantic: sources, transport, and relation to oceanography. *Marine Geology* **130**, 203–229.

Pirrung B. M. (1998) Zur Entstehung isolierter alttertiärer Seesedimente in zentraleuropäischen Vulkanfeldern. *Mainzer naturw. Arch.* **44**, 61-70.

Poschmann, M., Schindler, T. and Uhl, D. (2010) Fossil-Lagertsätte Enspel - a short review of current knowledge, the fossil association, and a bibliography. *Palaeobiodiversity and Palaeoenvironments* **90**, 3-20.

Rasmussen B., Fletcher I. R., Brocks J. J. and Kilburn M. R. (2008) Reassessing the first appearance of eukaryotes and cyanobacteria. *Nature* **455**, 1101-1104.

Rubinstein I., Sieskind O. and Albrecht P. (1975) Rearranged sterenes in a shale: occurence and simulated formation. *Journal of Chemical Society, Perkin Transaction I*, 1833-1836.

Rullkötter J. and Marzi R. (1988) Natural and artificial maturation of biological markers in a Toarcian shale from northern Germany. *Org. Geochem.* **13**, 639-645.

Rullkötter, J., and Isaacs, C. M. (2001) Compilation of geochemical data and analytical methods: Cooperative Monterey organic geochemistry study. In: The Monterey Formation From Rocks to Molecules (eds. Isaacs, C.M. and Rullkötter, J.), pp. 399-460.

Schindler, T. and Wuttke, M. (2010) Geology and limnology of the Enspel Formation, (Chattian, Oligocene; Westerwald, Germany). *Palaeobiodiversity and Palaeoenvironments* **90**, 21-27.

Schindler, T. and Wuttke, M. (2015) A revised sedimentological model for the late Oligocene crater lake Enspel (Enspel Formation, Westerwald Mountains, Germany). *Palaeobiodiversity and Palaeoenvironments* **95**, 5-16.

Schwark L., Stoddart D., Keuser C., Leythaeuser D. (1997) A novel sequential extraction system for whole core plug extraction in a solvent flow through cell

– application to extraction of residual petroleum from an intact pore system in secondary migration studies. *Org. Geochem.* **26**, 19-32.

Sepùlveda J., Wendler J. E., Summons R. E. and Hinrichs K.-U. (2009) Rapid Resurgence of Marine Productivity After the Creatceous-Paleogene Mass Extinction. *Science* **326**, 129-132.

Seifert W. K. and Moldowan J. M. (1978) Applications of steranes, terpanes and monoaromatics to the migration and source of crude oils. *Geochim. Cosmochim. Acta* **42**, 77–95.

Seifert W. K. and Moldowan J. M. (1980) The effect of thermal stress on source-rock quality as measured by hopane stereochemistry. *Physics and Chemistry of the Earth* **12**, 229–237.

Sherman L., Waldbauer J. and Summons R. E. (2007). Improved methods for isolating and validating indigenous biomarkers in Precambrian rocks. *Org. Geochem.* **38**, 1987–2000.

Sieskind O., Joly G. and Albrecht P. (1979) Simulation of the geochemical transformation of sterols: superacid effect of clay minerals. *Geochim. Cosmochim. Acta* **43**, 1675-1679.

Sinninghe Damsté J. S., Kok M. D., Köster J. and Schouten S. (1998) Sulfurized carbohydrates: an important sedimentary sink for organic carbon? *Earth Planet. Sci. Let.* **164**, 7–13.

Smith J. W., Schopf J. W. and Kaplan I. R. (1970) Extractable organic matter in Precambrian cherts. *Geochim. Cosmochim. Acta* **34**, 659–675.

Stankiewicz B. A., van Bergen P. F., Duncan I. J., Carter J. F., Briggs D. E. G. and Evershed R. P. (1996) Recognition of chitin and proteins in invertebrate cuticles using analytical pyrolysis-gas chromatography and pyrolysis-gas chromatography/mass spectrometry. *Rapid Comm. Mass Spectrom.* **10**, 1747-1757.

Stankiewicz, B. A., Briggs, D. E. G., Evershed, R. P., Flannery, M. B. and Wuttke, M. (1997) Preservation of chitin in 25 million-year-old fossils. *Science* **276**, 1541-1543.

Storch G., Engesser B. and Wuttke M. (1996) Oldest fossil record of gliding in rodents. *Nature* **379**, 439–441.

Subroto E. A., Alexander R. and Kagi R. I. (1991) 30-Norhopanes: their occurrence in sediments and crude oils. *Chem. Geol.* **93**, 179-192

Subroto E. A., Alexander R., Pranjoto U. and Kagi R. I. (1992) The use of 30-norhopane series, a novel carbonate marker, in source rock to crude oil correlation in the North Sumatra basin. *Proceedings of the Indonesian Petroleum Association 21st Annual Convention*, 145-163.

Taylor G. H., Teichmüller M., Davis A., Diessel C. F. K., Littke R. and Robert P. (1998) Organic Petrology. Gebrüder Bornträger, Berlin, Stuttgart, 704 pp.

Tegelaar E., de Leeuw J. W., Derenne S. and Largeau C. (1988) A reappraisal of kerogen formation. *Geochim. Cosmochim. Acta* **53**, 3103-3106.

ten Haven H. L., de Leeuw J. W., Rullkötter J. and Sinninghe Damsté J. S. (1987) Restricted utility of the pristine/phytane ratio as a paleoenvironmental indicator. *Nature* **330**, 641-643.

ten Haven H. L., de Leeuw J. W., Sinninghe Damste J. S., Schenck P. A., Palmer S. E., andZumberge J. E. (1988) Application of biological markers in the recognition of palaeo-hypersaline environments, In Lacustrine Petroleum Source Rocks: Special Publication (eds. K. Kelts, A. Fleet, and M. Talbot), Geological Society, London, pp. 123-130.

Tissot B. P. and Welte D. H. (1984) Petroleum formation and occurrence. Springer Verlag, Berlin. 699 pp.

Traverse A. (1988) Paleopalynology. Unwin Hyman, Boston. 600pp.

Uguna C. N., Carr A. D., Snape C. E., Meredith W., Scotchman I. C., Murray A. and Vane C. H. (2016) Impact of high water pressure on oil generation and maturation in Kimmeridge Clay and Monterey source rocks: Implications for petroleum retention and gas generation in shale gas systems. *Mar. Petrol. Geol.* **73**, 72-85.

Vandenbroucke M. and Largeau C. (2007) Kerogen origin, evolution and structure. *Org. Geochem.* **38**, 719-833.

van Kaam-Peters H. M. E., Köster J., van der Gaast S. J., Dekker M., de Leeuw J. W. and Sinnighe Damsté J. S. (1998) The effect of clay minerals on diasterane/sterane ratios. *Geochim. Cosmochim. Acta* **62**, 2923-2929.

van Krevelen D. W. (1993) Coal: Typology - Chemistry - Physics – Constitution. Elsevier Science and Technology, 1000 pp.

Vogt, C., Lauterjung, J. and Fischer, R.X. (2002) Investigation of the clay fraction (<2 μm) of the clay mineral society reference clays. Clays and Clay Minerals, **50**, 388-400.

Waldbauer J. R., Sherman L. S., Sumner D. Y. and Summons R. E. (2008). Late Archean molecular fossils from the Transvaal Supergroup record the antiquity of microbial diversity and aerobiosis. *Precambr. Res.* **169**, 28–47.

Wakeham S. G. (1990) Algal and bacterial hydrocarbons in particulate matter and interfacial sediment of the Cariaco Trench. *Geochim. Cosmochim. Acta* **54**, 1325-1336.

Wilhelms A., Larter S. R. and Leythaeuser, D. (1991) Influence of bitumen-2 on Rock-Eval pyrolysis. *Org. Geochem.* **17**, 351–354.

Williford K. H., Ushikubo T., Lepot K., Kitajima K., Hallmann C., Spicuzza M. J., Kozdon R., Eigenbrode J. L., Summons R. E. and Valley J. W. (2016) Carbon and sulfur isotopic signatures of ancient life and environment at microbial scale: Neoarchean shales and carbonates. *Geobiology* **14**, 105-128.

FIGURE CAPTIONS

Figure 1: Stratigraphy of the sampled outcrop and bulk geochemical parameters. The lava contact is set at 0 cm and sample levels are labeled. Profiles for reflectance (%$R_{O\ mean}$), total organic carbon (TOC) content, the TOC/TN ratio, T_{max} (solid line: bulk; dashed line: extracted sample) and aromaticity (δ) are plotted against stratigraphy, demonstrating a trend of increasing thermal maturity towards the top.

Figure 2: Extraction scheme illustrating laboratory workflow. The three different successive extraction methods (ULTRA, ASE, B2) are color-coded.

Figure 3: ^{13}C NMR spectra for organic matter in Level 2 (nearest to lava flow; R_O mean based on two measurements = 1.07 %) and Level 14 (farthest away from the lava flow; R_O mean = 0.25 %). Yellow peak corresponds to carbon in aromatic structures (peak of 119.555 ppm in Level 2) and blue (peak of 40.651 ppm in Level 2 and 28.584 ppm in Level 14) to carbon in alkyl groups.

Figure 4: Light microscope photographs of thin sections and particulate organic matter preparations of Levels 12, 6 and 2 illustrate the color change of organic matter with decreasing distance from the lava flow. R_O mean (%) and the palynological organic matter color (visually estimated with reference to color chart in Traverse, 1988) are given as measures of the degree of thermal maturity.

Figure 5: Extraction efficiency in relation to thermal maturity. A) Relative extract yield obtained by ULTRA, ASE and B2, normalized to the summed total extract yield. B) Extraction efficiency of individual ASE extraction steps, normalized to the combined total ASE yield. C) Absolute extract yield of the ULTRA, ASE and B2 (left y axis) and the individual ASE fractions (right y axis) showing a decrease with progressive extractions D) TLE yields normalized to sample weight.

Figure 6: Chromatograms (GC-MS; *m/z* 85) showing the distribution of *n*-alkanes in free (left traces: ULTRA) and occluded bitumens (right traces: B2). Black circle indicates *n*-C_{27}. The maximum peak of each chromatogram is indexed. To visualize the change in composition, the B2 *m/z* 85 trace is plotted over a shaded sketch of the ULTRA *n*-alkane distribution. Plots are scaled to individual maximum peaks. Thermal stress is increasing towards the top.

Figure 7: Reconstructed ion chromatograms (GC-MRM-MS: *m/z* 191) of ULTRA and B2 extracts of Levels 2 (R_O = 1.07 %), 6 (R_O = 0.50 %) and 12 (R_O = 0.25 %). Chromatograms are reconstructed from parent-daughter reactions: *m/z* 370, 384, 398, 412, 426, 440, 454, 468 and 482 to *m/z* 191. Homologous series of αβ (red circles)

and ββ (green; triangles) hopanes and moretanes (blue diamonds) are indexed. For position of samples see Figs. 1 and 6.

Figure 8: Isomerization of C_{30}-hopanes (A) and relative abundance of C_{27}-, C_{28}- and C_{29}-sterane homologs (B) in ULTRA, ASE1 and B2 extracts of increasing thermal maturity (from Level-14 to Level-2).

Figure 9: Chromatograms (GC-MRM-MS transition *m/z* 386 to 217) showing C_{28} steranes in ULTRA and B2 extracts of Levels-2 (R_O = 1.07 %), -6 (R_O = 0.50 %) and -12 (R_O = 0.25 %). Peaks were identified in comparison to the AGSO laboratory standard. Note the similar thermal maturity but differences in the relative abundance of diasteranes between ULTRA and B2. See Figs. 1 and 6 for the stratigraphic position of samples.

Figure 10: Composite plot modified after Peters et al. (2005) showing biomarker response to thermal maturation (black bars) and the observed range (minimum to maximum) in ULTRA (red range) and B2 (blue range). The observed range of spore color index and vitrinite reflectance (% R_O) is shown in relation to the oil generative window.

Figure 11: Changes in average chain length (ACL), carbon preference index (CPI-1; cf. Peters et al., 2005), pristane-phytane ratio (Pr/Ph) and the C_{29} dia/regular sterane ratio plotted against stratigraphic height.

Figure 12: Typical hopane ratios indicative of thermal maturity in ULTRA, ASE and B2 plotted against stratigraphic height.

Figure 13: Isomerization ratios of C_{27}-, C_{28}- and C_{29}-steranes in ULTRA and B2 extracts plotted against stratigraphic height.

Table 1: Elemental composition (wt.%), T_{MAX} (°C) of bulk and extracted samples, as well as, ^{13}C NMR aromaticity of bulk rock samples. (Total Organic Carbon (TOC) is calculated from Total Carbon (TC) – Total Inorganic Carbon (TIC); *n.d.* = not determined).

Table 2: Palynological organic matter color and average vitrinite reflectance values of the seven shale levels, indicating increasing thermal maturity of the organic matter in proximity to the basalt flow.

Table 3: Results of the Rock Eval measurements (T_{MAX} in °C; S1, S2, S3 are given in mg hydrocarbons/g rock; *n.d.* = not determined).

Table 4: Mineralogical composition of the examined samples determined by x-ray diffraction, results are given in weight %. (Qtz: quartz; Plag: plagioclase; Carb: carbonates; Py: pyrite; Fe-ox: iron oxides; Expandable clays are a sum of; MO: montmorillinite; SM: smectite; MX: mixed-layer clays; IL: illite; MI: mica)

Figure 1

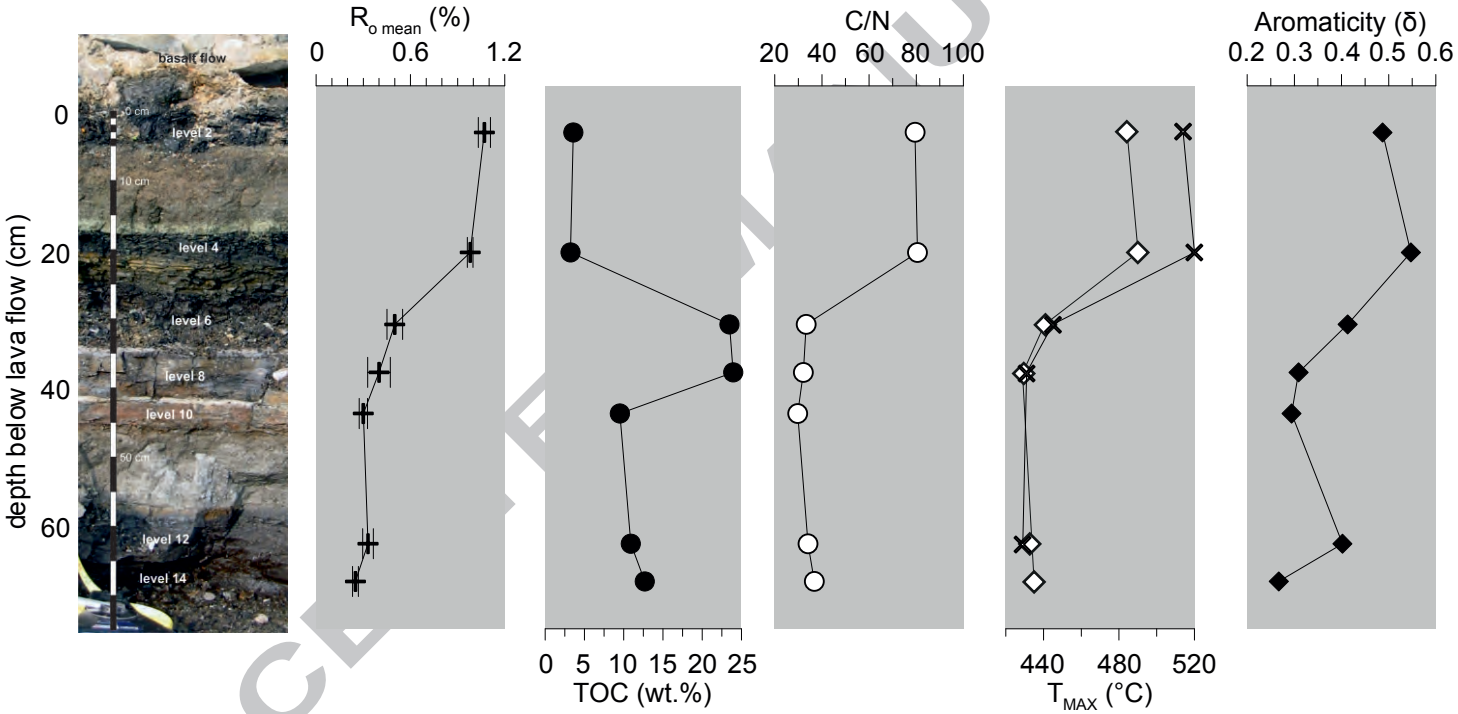

Figure 2

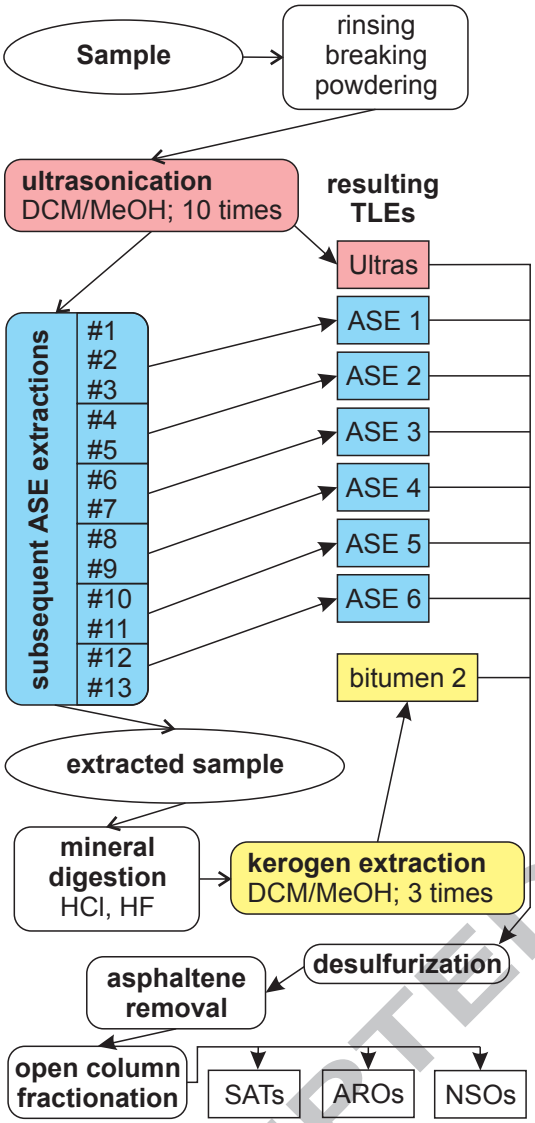

Figure 3

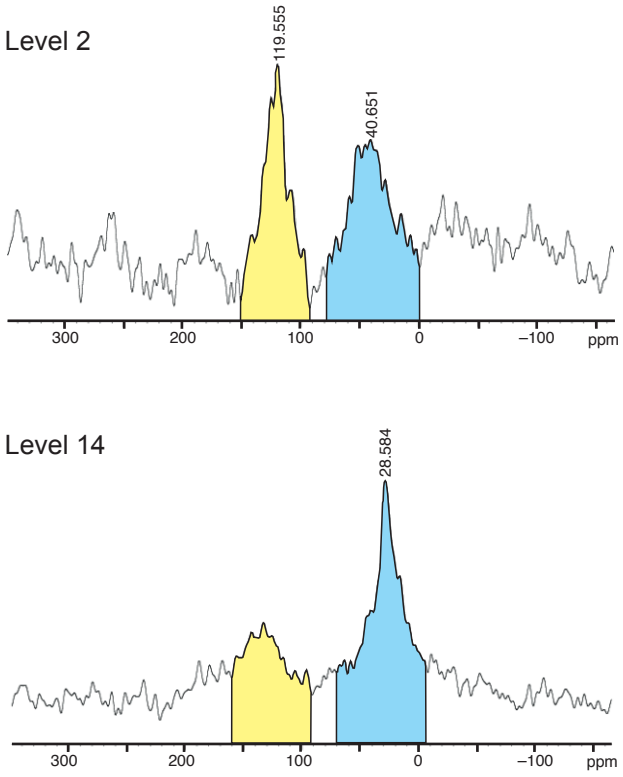

Figure 4

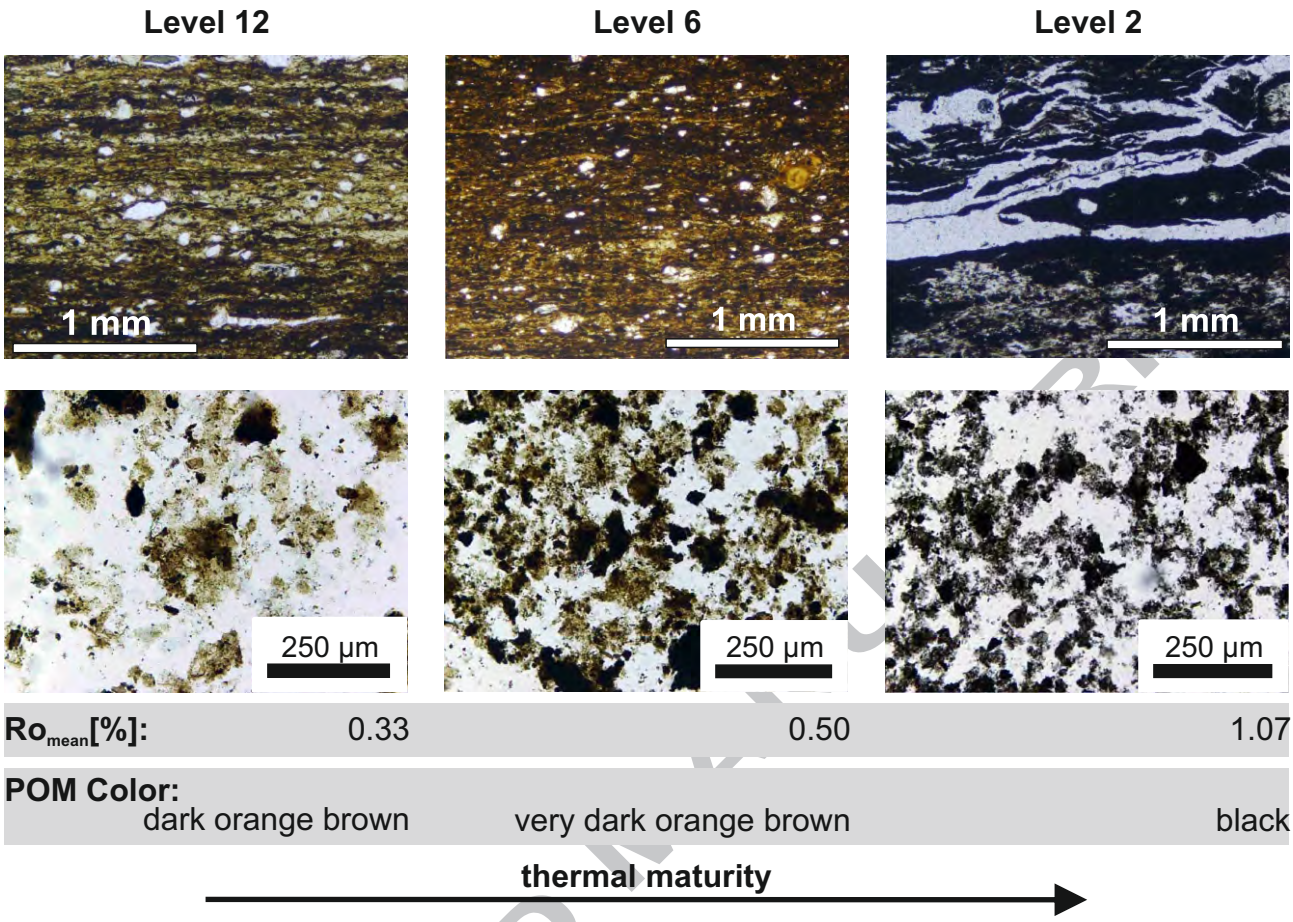

Figure 5

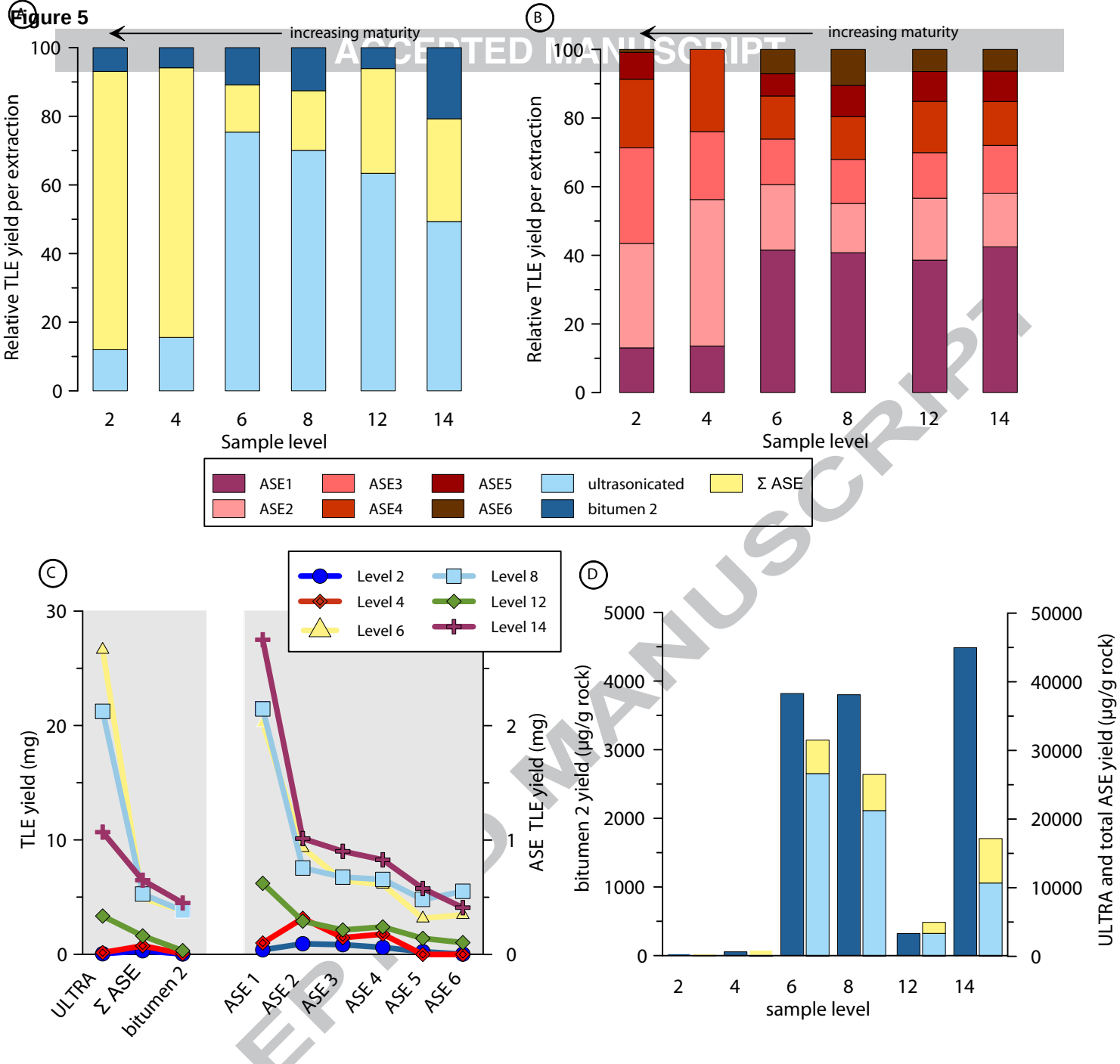

Figure 6

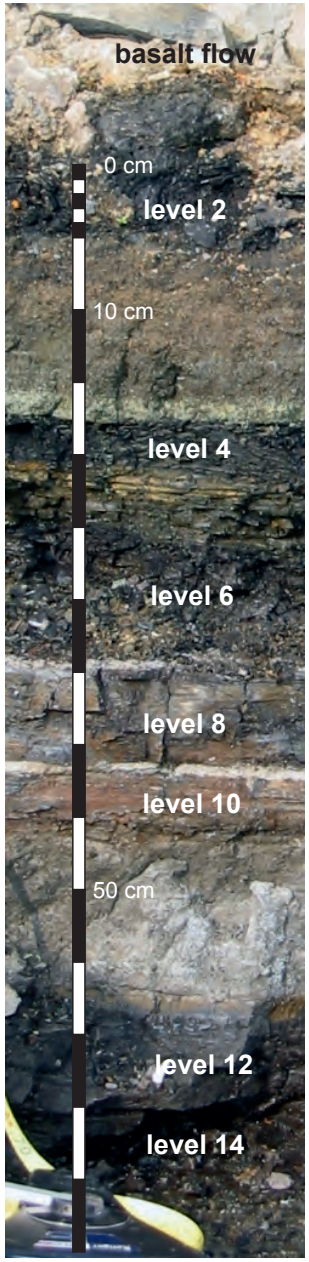

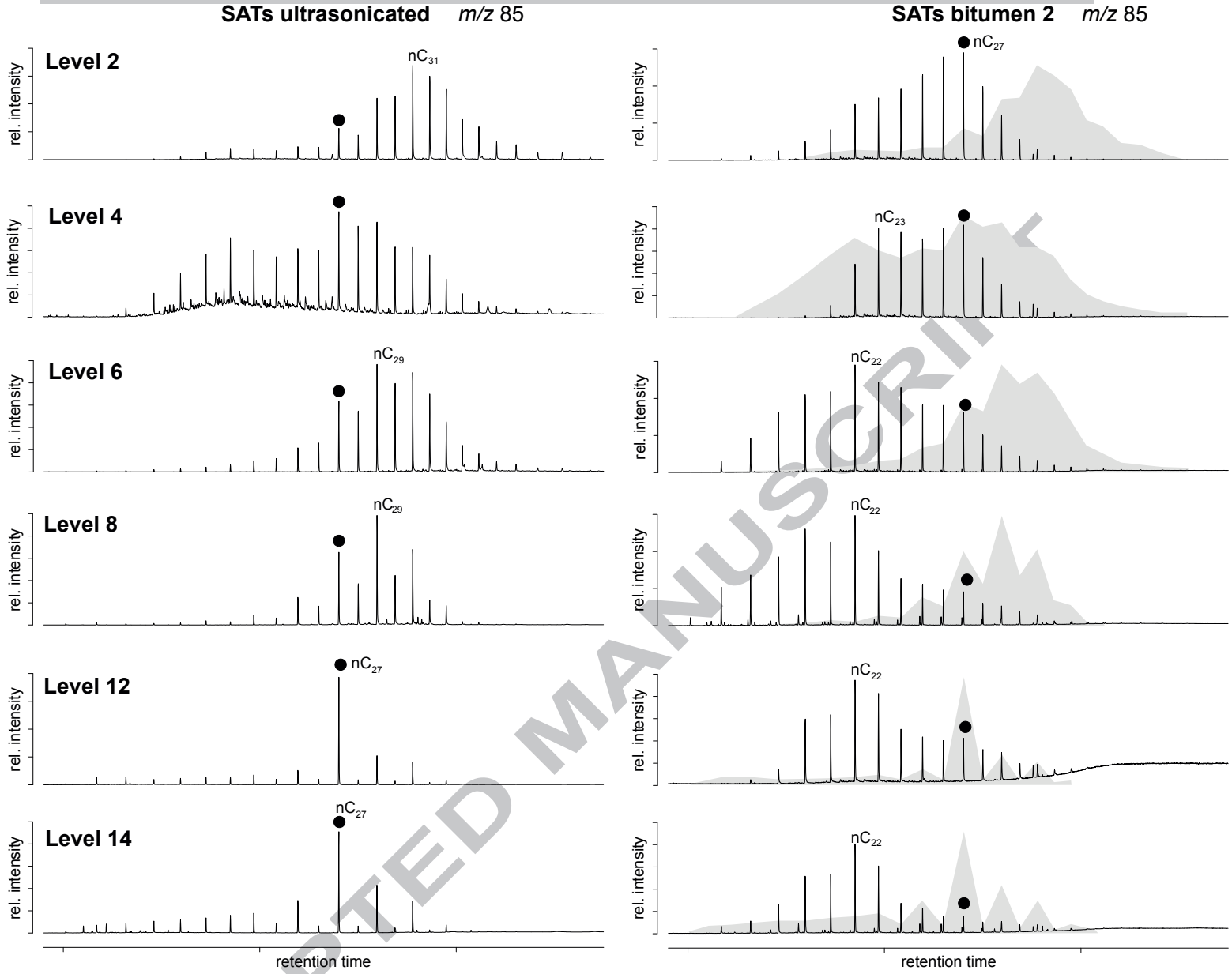

Figure 7

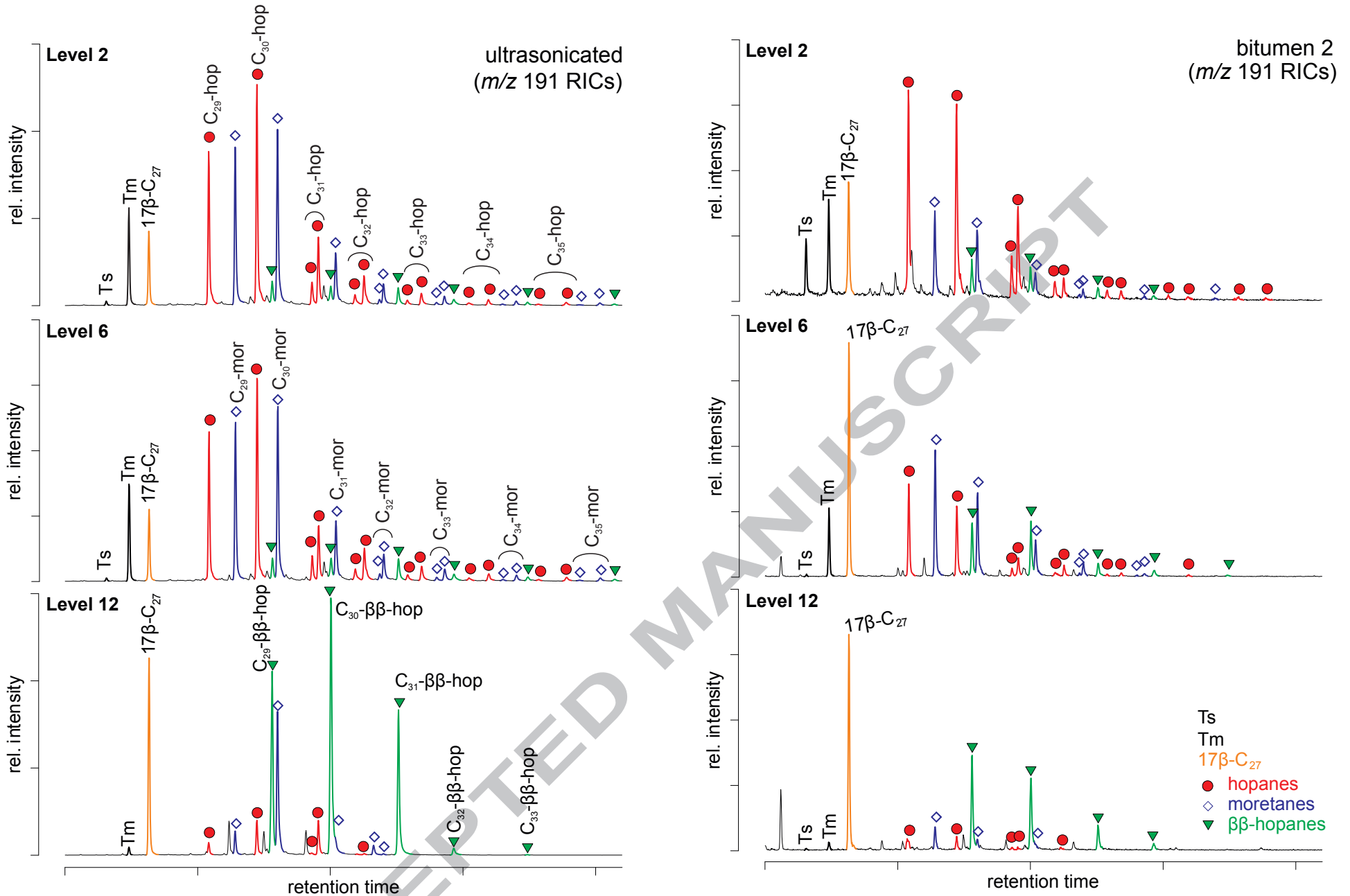

Figure 8

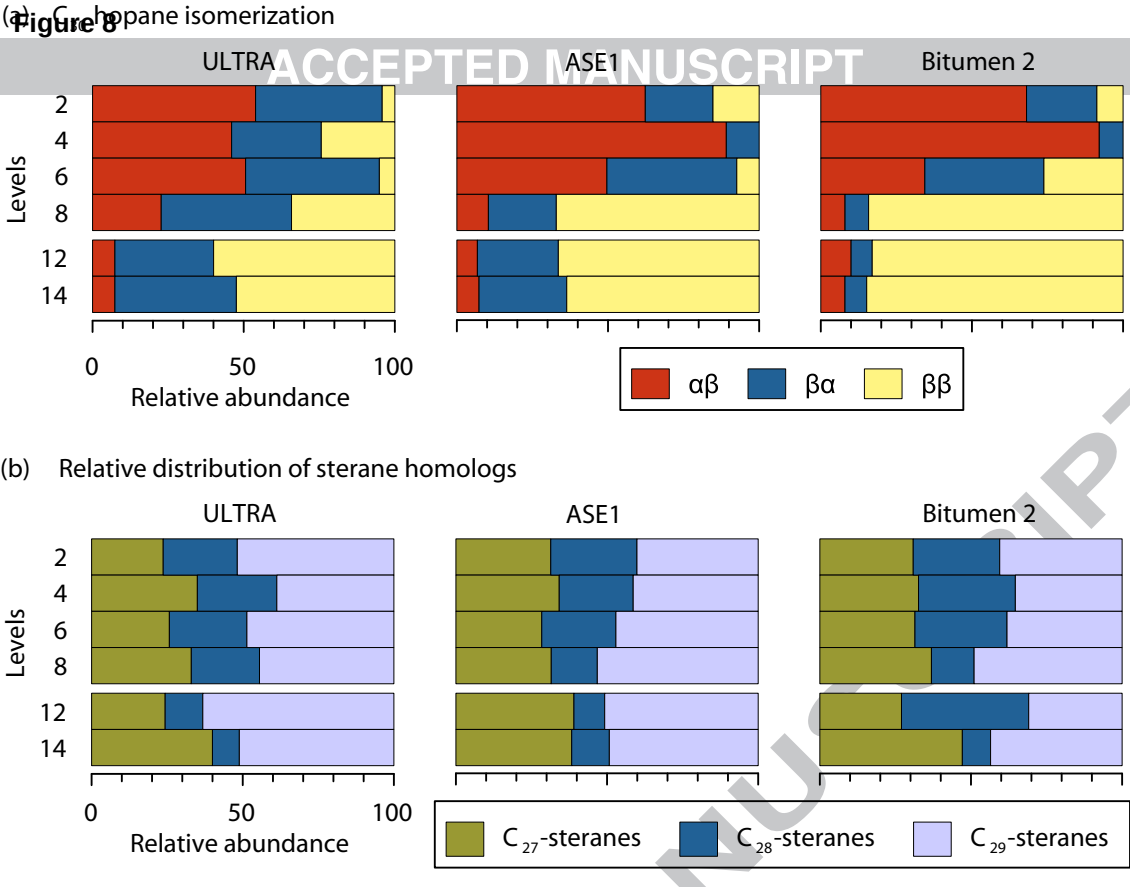

Figure 9

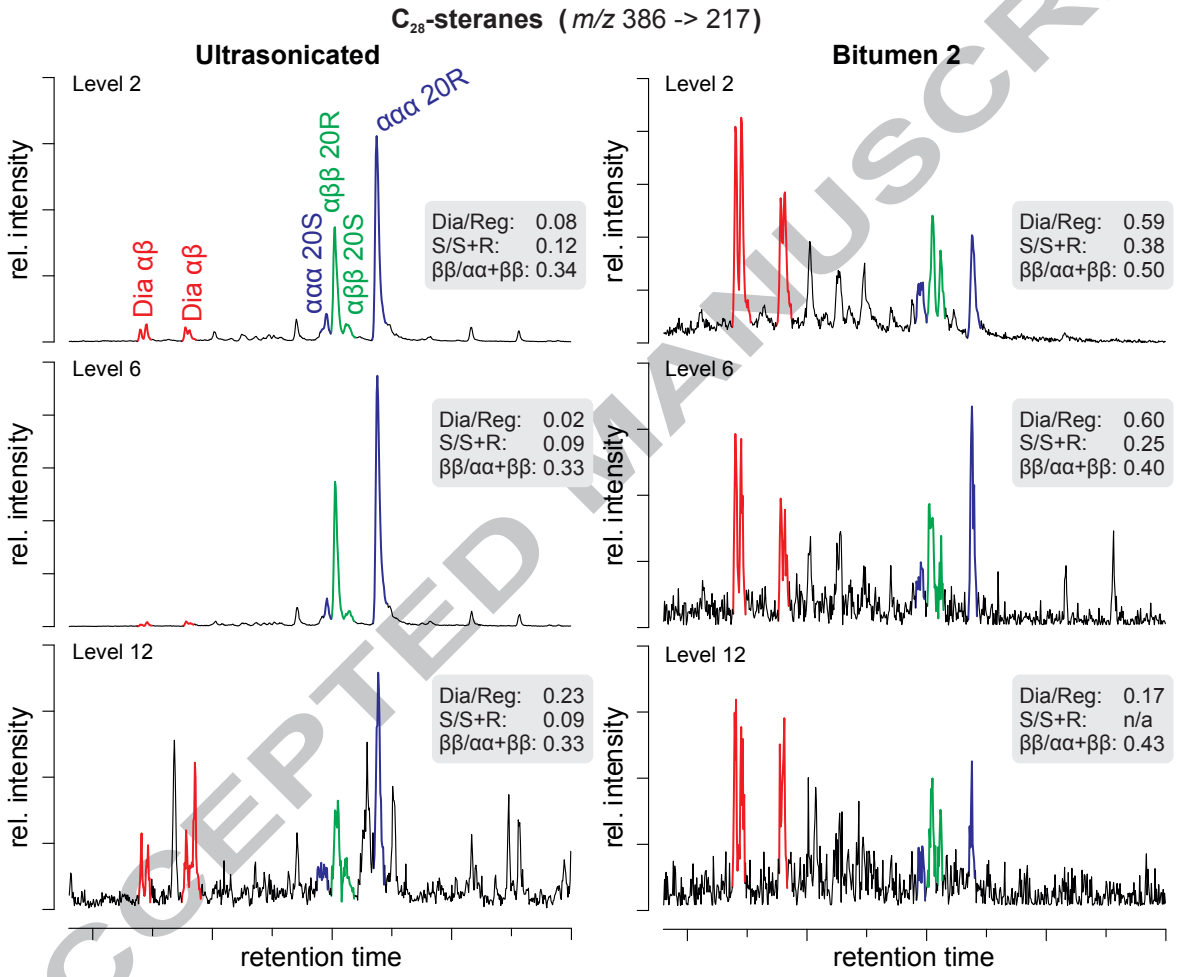

Figure 10

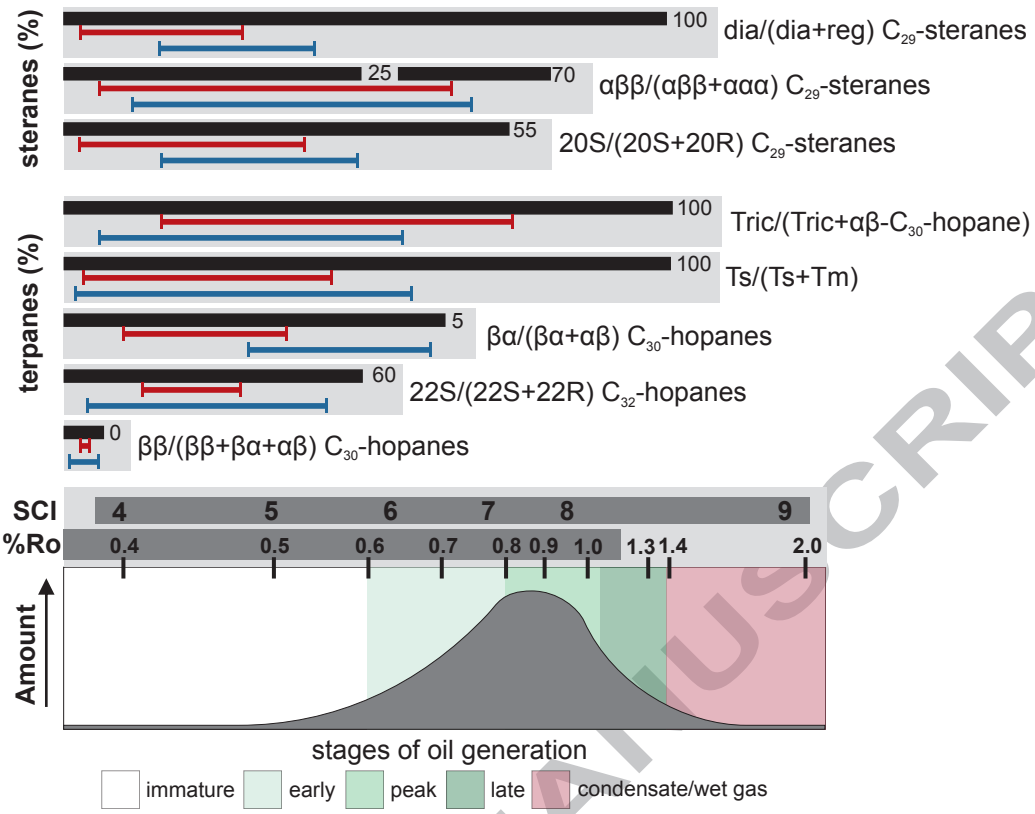

Figure 11

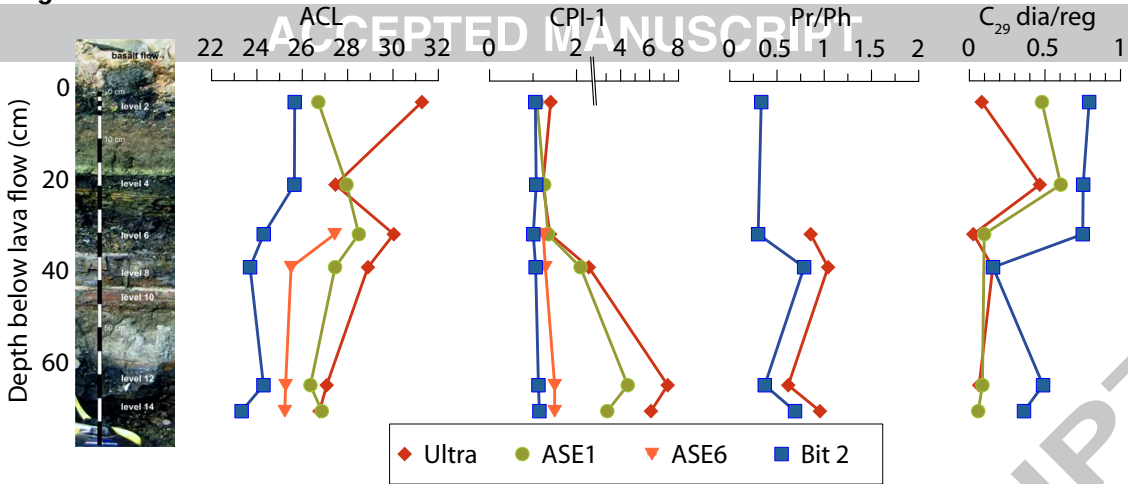

Figure 12

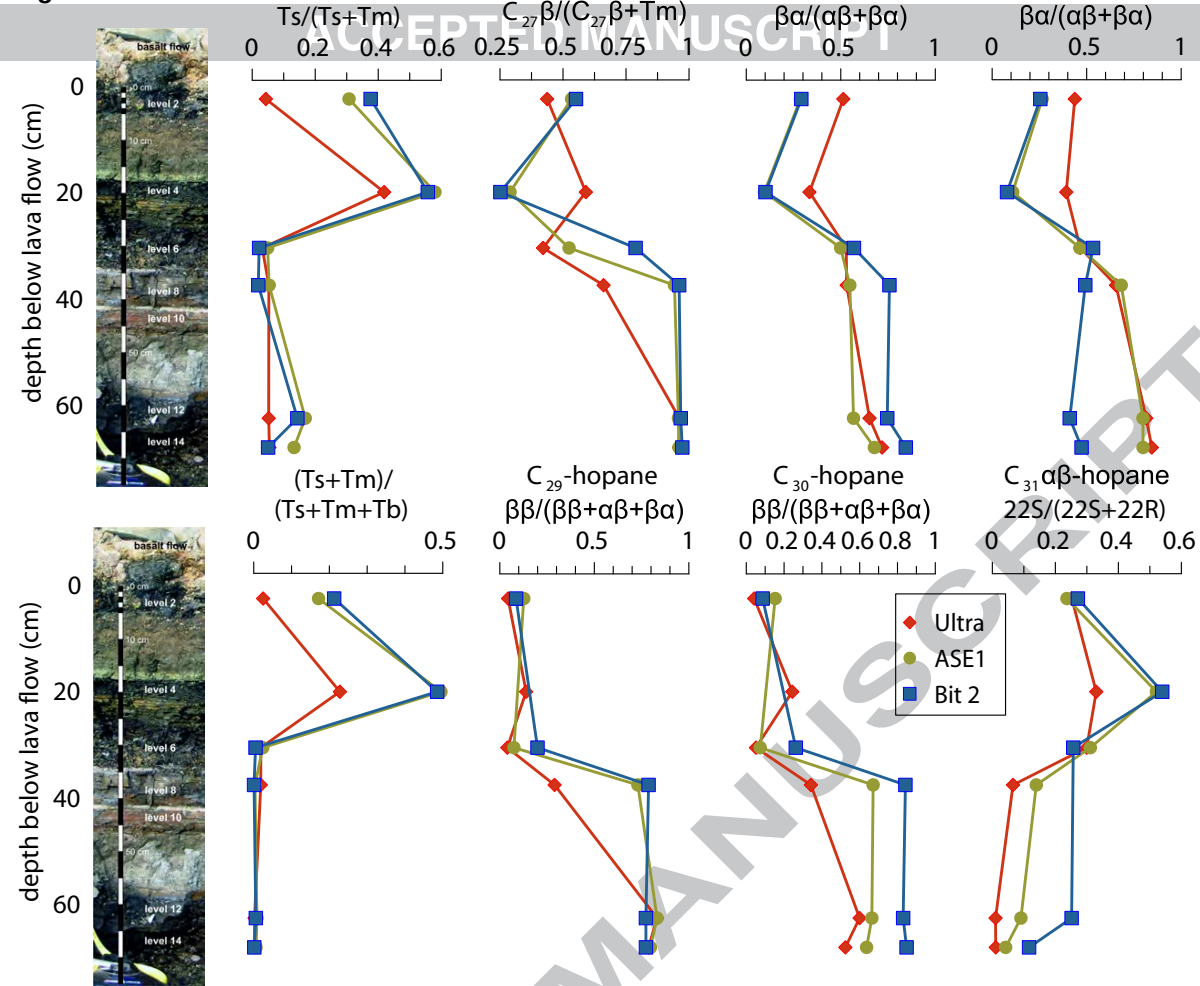

Figure 13

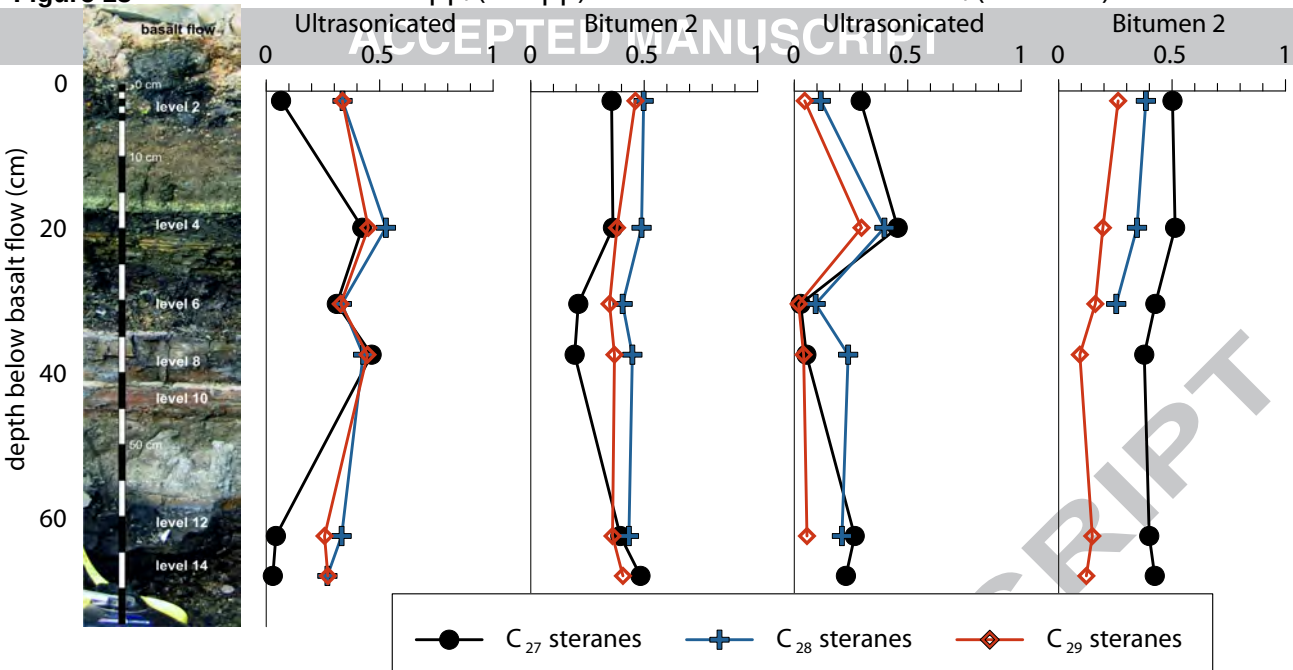

Table 1: Elemental composition (wt.%), T_{MAX} (°C) of bulk and extracted samples, as well as, ^{13}C NMR aromaticity of bulk rock samples. (Total Organic Carbon (TOC) is calculated from Total Carbon (TC) – Total Inorganic Carbon (TIC); *n.d.* = not determined).

Level	TC [wt.%]	TIC [wt.%]	TOC [wt.%]	TN [wt.%]	C/N	T_{MAX} [°C] bulk/extracted	Aromaticity (δ)
2	3.6	0.02	3.6	0.05	79	514 / 484	0.49
4	3.2	0.02	3. 2	0.04	81	520 / 490	0.55
6	23.5	0.02	23.5	0.71	33	445 / 442	0.41
8	24.0	0.03	24.0	0.75	32	431 / 429	0.31
10	9.5	0.02	9.5	0.32	30	*n.d.* / *n.d.*	0.29
12	10.9	0.03	10.9	0.32	34	429 / 432	0.40
14	12.7	0.04	12.7	0.35	37	*n.d.* / 435	0.27

Table 2: Palynological organic matter color and average vitrinite reflectance values of the seven shale levels, indicating increasing thermal maturity of the organic matter in proximity to the basalt flow.

Level	Spore Color Index	Color	Average R_o (%)
2	9–10	Black	1.07 ± 0.05
4	8–9	Very dark brown	0.98 ± 0.07
6	7	Very dark orange brown	0.50 ± 0.03
8	4–5	Dark orange-brown	0.40 ± 0.04
10	4	Orange-brown	0.30 ± 0.02
12	4–5	Dark orange-brown	0.33 ± 0.02
14	4	Orange-brown	0.25 ± 0.03

Table 3: Results of the Rock Eval measurements (T_{MAX} in °C; S1, S2, S3 are given in mg hydrocarbons/g rock; *n.d.* = not determined).

Level	S1	S2	S3	T_{MAX}	S1	S2	S3	T_{MAX}
	Unextracted				*Extracted*			
2	0.01	0.03	2.05	514	0.02	0.03	0.78	484
4	0.01	0.04	3.58	520	0.11	0.11	3.22	490
6	0.37	67.45	2.46	445	0.7	75.5	4.44	442
8	3.28	151.14	9.84	431	1.95	124.51	10.63	429
12	0.32	22.14	2.73	429	0.25	13.39	2.56	432
14	*n.d.*	*n.d.*	*n.d.*	*n.d.*	1.32	69.91	9.2	435

Table 4: Mineralogical composition of the examined samples determined by x-ray diffraction, results are given in weight %. (Qtz: quartz; Plag: plagioclase; Carb: carbonates; Py: pyrite; Fe-ox: iron oxides; Expandable clays are a sum of; MO: montmorillinite; SM: smectite; MX: mixed-layer clays; IL: illite; MI: mica)

Level	Qtz	Plag	Carb	Py	Fe-ox	Exp. Clays *	Others	*MO+ SM	*MX	*IL+ MI
								Phyllosilicates		
2	49.8	3.4	2.2	0.0	0.0	36.0	8.7	35.6	0.4	0.0
4	2.4	1.0	1.0	0.0	15.9	63.6	16.2	32.6	3.6	27.4
6	8.3	13.5	2.6	1.8	0.5	56.4	16.9	38.3	5.2	13.0
8	9.6	6.7	0.0	3.8	1.4	62.5	16.0	13.5	20.3	28.7
12	26.9	11.2	0.0	0.0	1.9	45.0	15.0	3.8	23.4	17.8
14	12.1	16.7	0.0	4.7	1.8	45.7	19.0	34.7	7.9	3.1